

N O T I C E

THIS DOCUMENT HAS BEEN REPRODUCED FROM
MICROFICHE. ALTHOUGH IT IS RECOGNIZED THAT
CERTAIN PORTIONS ARE ILLEGIBLE, IT IS BEING RELEASED
IN THE INTEREST OF MAKING AVAILABLE AS MUCH
INFORMATION AS POSSIBLE

SEMI-ANNUAL STATUS REPORT

(Period Covered: February 1, 1981 - July 31, 1981)

A COMPREHENSIVE MODEL TO DETERMINE THE EFFECTS
OF TEMPERATURE AND SPECIES FLUCTUATIONS ON
REACTION RATES IN TURBULENT REACTING FLOWS*



P.J. Antaki, G. Ronan, E. Foy and W. Chinitz**
The Cooper Union Research Foundation, Inc.
New York, New York 10003

(NASA-CR-164552) A COMPREHENSIVE MODEL TO
DETERMINE THE EFFECTS OF TEMPERATURE AND
SPECIES FLUCTUATIONS ON REACTIONS IN
TURBULENT REACTING FLOWS Semiannual Status
Report (Cooper Union) 51 p HC A04/MF A01 G3/02 26755
N81-27039
Unclass

*Work supported under Grant No. NAG1-18, National Aeronautics and Space Administration, Langley Research Center, High-Speed Aerodynamics Division, Hypersonic Propulsion Branch, Hampton, VA 23665

**Principal Investigator

TABLE OF CONTENTS

	<u>PAGE</u>
1. Introduction	
2. The Modified Bivariate Gaussian PDF	1
3. The "Most-Likely" PDF	13
4. A Criterion for Selecting a Temperature PDF in Turbulent Flows	16
5. Discussion of Alternative Models for the Determination of Reaction Rates in Turbulent Reacting Flows	20
References	27
List of Symbols	29
Figures	

1. Introduction

In this semi-annual status report, the work previously - initiated ⁽¹⁾ dealing with the joint pdf which is a modification of the bivariate Gaussian pdf is discussed in detail and results are presented for a global reaction model using this joint pdf (Section 2). An alternative joint pdf, the "most-likely" pdf, suggested by Pope ⁽²⁾, is discussed in Section 3. A criterion is developed in Section 4 which permits the selection of temperature pdf's in different regions of turbulent, reacting flow fields. Section 5 sets forth two principal approaches to the determination of reaction rates in computer programs containing detailed chemical kinetics. These models are set forth in the context of current research in this field and, it is argued, represent a practical solution to the modeling of species reaction rates in turbulent, reacting flows.

2. The Modified Bivariate Gaussian PDF

Numerous experimental studies are available which describe pdf's for temperature in both non-reacting and reacting turbulent flows. A number of these (eg, "clipped" Gaussian, beta, ramp) have been discussed previously. However, no experimental studies are available describing joint pdf's of temperature and species in any flow. The bivariate, or two dimensional, Gaussian pdf has been chosen as a joint pdf which has at least a conceptual basis in physical reality. This conclusion is drawn by imagining the behavior of the marginal pdf's of temperature and species, each a one-dimensional Gaussian pdf, during the course of a reaction. The marginal pdf's show that the mean temperature can be low while the mean concentration of fuel, for example, is high. This could correspond to an initial stage of a reaction. As the reaction proceeds, the mean temperature increases as the mean concentration of fuel decreases. The marginal pdf's can exhibit this behavior. Based on this presumed physical behavior, it is assumed that the bivariate Gaussian pdf serves as a reasonable approximation to the actual joint pdf of temperature and species in a turbulent reacting flow. This is intended as an initial step in the formulation of such pdf's.

The form of the bivariate Gaussian pdf is (1)

$$p(t, x) = \frac{1}{2\pi\sigma_t\sigma_x\sqrt{1-\rho^2}} \cdot \exp\left\{-\frac{1}{2(1-\rho^2)}\left[\frac{(t-\mu_t)^2}{\sigma_t^2} - \frac{2\rho(t-\mu_t)(x-\mu_x)}{\sigma_t\sigma_x} + \frac{(x-\mu_x)^2}{\sigma_x^2}\right]\right\} \quad (1)$$

for $-\infty < t < \infty$, $-\infty < x < \infty$, and where ρ is the correlation coefficient between t and x .

The bivariate Gaussian pdf is valid on the interval of minus to plus infinity for both variables and as such, cannot be utilized in its present form. To remedy this situation, the pdf is modified as follows. Let

$$v = \int_0^1 \int_0^1 p(t, x) dt dx \quad (2)$$

It follows that,

$$f(t, x) = \frac{1}{v} p(t, x) \quad \begin{cases} 0 \leq t \leq 1 \\ 0 \leq x \leq 1 \end{cases} \quad (3)$$

which is the form of the modified bivariate Gaussian pdf. This pdf is a valid one, as it satisfies the condition required of a pdf.

Equation (5) below is a general expression for the reaction rate of fuel for any particular one-step, irreversible reaction of the form:



from which

$$\dot{w}_F = K(t) (x_F c_F^0)^n (x_O c_O^0)^m \quad (5)$$

where

$$x_i \equiv \frac{c_i - c_{i,MIN}}{c_{i,MAX} - c_{i,MIN}} = \frac{c_i}{c_i^0}$$

for the fuel and the oxidizer.

That is, x_F and x_0 are dimensionless concentrations that are bounded by zero and one. The terms c_F^0 , c_0^0 represent the initial concentrations of fuel and oxidizer, respectively, and n and m are constants. By assuming that n and m are both equal to unity, it is possible to rewrite (5) as

$$\dot{w}_F = -K(t) x_F c_F^0 \left[\nu c_F^0 (x_F - 1) + c_0^0 \right] \quad (6)$$

Therefore, \dot{w}_F is a function of two variables, t and x_F . Equation (6) can be used along with the modified bivariate Gaussian pdf to determine the mean turbulent reaction rate. That is,

$$\overline{\dot{w}_t} = -A_0 \int_0^1 \int_0^1 (k_1 t + k_2)^B \cdot \exp \left[-T_A / (k_1 t + k_2) \right] \cdot x_F c_F^0 \left[\nu c_F^0 (x_F - 1) + c_0^0 \right] \cdot p(t, x_F) dt dx_F / \int_0^1 \int_0^1 p(t, x_F) dt dx_F \quad (7)$$

where:

$p(t, x_F)$ is given by eq (1).

For a given or calculated mean turbulent reaction rate, the corresponding laminar term can be determined by inserting the proper values of \bar{t} and \bar{x}_F , the mean dimensionless temperature and mean dimensionless concentration of fuel, respectively, into eq (6). The reaction rate amplification ratio is then:

$$Z' = \frac{\overline{\dot{w}_t}}{\dot{w}_L} \quad (8)$$

This reaction rate amplification ratio considers the combined effects of temperature and species fluctuations on the reaction rate. As described in ref 1, Section 3(a), the assumption of statistical independence between temperature and species fluctuations leads to

$$Z' = \frac{\overline{K_e}}{K_e} = Z \quad (9)$$

Amplification ratios calculated with both eqs (8) and (9) can be compared to determine the effect of the inclusion of species fluctuations on the reaction rate, in addition to the temperature effect. For purposes of a parameter study, the following one-step, irreversible reaction is considered:



The data of ref 3 are utilized to determine an approximate relationship between the dimensionless mean temperature and the dimensionless mean concentration of hydrogen in a turbulent diffusion flame. Shown in figure 1 are curve fits of data from ref 3, (fig 2, $\overline{U}_j/U_e = 8$). The mean temperature is non-dimensionalized by use of the values of $T_{\max} = 2160\text{K}$ and $T_{\min} = 300\text{K}$. The range of data for which the temperature is decreasing is ignored as it is assumed to be the result of heat transfer. In a hypothetical adiabatic system, this heat transfer would not occur. From the figure, it is readily determined that an approximate relationship between \overline{t} and $\overline{x_{\text{H}_2}}$ is:

$$\overline{x_{\text{H}_2}} = 1 - \overline{t} \quad (10)$$

This is deemed adequate for purposes of this parameter study.

Assume that in the radial direction of a confined axisymmetric turbulent diffusion flame, the Prandtl mixing length hypothesis is valid. Thus:

$$\sqrt{\overline{t'^2}} = L \left| \frac{d\bar{t}}{dy} \right| \quad ; \quad \sqrt{\overline{x_{H_2}'^2}} = L \left| \frac{d\bar{x}_{H_2}}{dy} \right|$$

where L = mixing length and y = radial coordinate.

Then

$$\frac{\overline{t'^2}}{\overline{x_{H_2}'^2}} = \frac{\left| d\bar{t}/dy \right|^2}{\left| d\bar{x}_{H_2}/dy \right|^2}$$

The following data are extracted from ref 3, ($\bar{U}_j/U_e = 10$, $X/D = 40$):

r/a	$\Delta\bar{t}/\Delta(r/a)$	$ \Delta\bar{r}/\Delta(r/a) $
1-2	0.08	0.05
2-3	0.17	0.07
3-4	0.24	0.11
4-5	0.22	0.21
5-6	0.21	0.23
6-6.1	0.30	0.30

Note: $r/a \sim y$

Averaging yields

$$\left| \frac{\overline{\Delta \bar{t}}}{\Delta y} \right| = 0.20 \quad \text{and} \quad \left| \frac{\overline{\Delta x_{H_2}}}{\Delta y} \right| = 0.16$$

Then

$$\frac{\overline{t'^2}}{\overline{x_{H_2}'^2}} = \frac{(0.20)^2}{(0.16)^2} = 1.56$$

Thus, $\overline{t'^2} = 3/2 \overline{x_{H_2}'^2}$ has been chosen for the purposes of this parameter study.

Figure 1 can also be utilized for the determination of the correlation coefficient, ρ , between temperature and species. The Statistics I Pac for the Hewlett Packard 41C programmable calculator was employed. This pac utilizes an approximate expression for the correlation coefficient.

Pairs of data points for \bar{t} and $\overline{x_{H_2}}$, at corresponding values of X/D up to approximately 130 were chosen. It was found that $\rho = -0.99$ is the value consistently calculated. It is assumed that this result is the same for instantaneous values of temperature and concentration. A similar procedure is followed with the use of data from ref 3, and identical results obtained. The results obtained using the modified bivariate Gaussian pdf, eqs (7) and (8) are compared with the reaction rate amplification ratio of eq (9), determined by use of the beta pdf, in which only the effect of temperature fluctuations on the reaction rate is considered. This amplification ratio is equivalent to the reaction rate constant amplification ratio utilizing the beta pdf presented in refs 1 and 4. A comparison of these two reaction rate amplification ratios allows the combined effects of temperature and species fluctuations to be compared

with the temperature fluctuation-only effect. The cases considered are those which involve the variation of the following: mean dimensionless temperature and mean species concentration, dimensionless temperature and species concentration fluctuations, the correlation coefficient, the relationship between $\overline{x_{H_2}^{T^2}}$ and $\overline{t^{T^2}}$, and the maximum temperature.

All numerical integrations were performed with the use of a Monte Carlo (random variable) technique. The number of random variables utilized is twenty-thousand (2×10^4). This number ensures that essentially no truncation error is incurred. There is a limit on the modified bivariate Gaussian's range of applicability, generally in the region of low temperature and species concentration fluctuations, as well as high mean temperature and correspondingly low mean species concentration. This is due both to the mathematical behavior of the function and the formulation of the model. These limitations are reflected in the results which follow.

Shown in Table 1. are the defining values and relationships for the cases considered. The initial values of concentration are taken from Test Case 1 of ref 5. All other constants are taken from ref 5 and are considered typical. Throughout this discussion, the use of the terms "temperature" and "concentration" denote mean dimensionless temperature and mean dimensionless species concentration, respectively.

Shown in figs . 2 through 6 are the results of the

Table 1 Case Data

Case No.	B	T_A (°K)	T_{max} (°K)	ρ	$\overline{x_{H_2}^{1/2}}$ vs. $\overline{t^{1/2}}$
1	0	10116	2500	-0.9	$\overline{x_{H_2}^{1/2}} = 2/3 \overline{t^{1/2}}$
4	0	10116	3000	-0.9	$\overline{x_{H_2}^{1/2}} = 2/3 \overline{t^{1/2}}$
5	0	10116	2500	-0.8	$\overline{x_{H_2}^{1/2}} = 2/3 \overline{t^{1/2}}$
6	0	10116	2500	-0.9	$\overline{x_{H_2}^{1/2}} = 1/2 \overline{t^{1/2}}$

Note: $A = 8.4 \times 10^{13}$, $T_{min} = 500^\circ K$, $C_{H_2}^0 = 2.405 \times 10^{-5} \text{ gmol/cm}^3$,

$C_{O_2}^0 = 1.5 \times 10^{-6} \text{ gmol/cm}^3$, $\overline{x_{H_2}} = 1 - \overline{t}$, for all cases

variation of the reaction rate amplification ratio with combined temperature and concentration fluctuations, at various constant values of temperature and concentration. Selected results of the temperature-only case (beta pdf) are shown for purposes of comparison.

Figs 2 and 3 show that at high temperatures and low concentrations, the amplification ratio of the combined case is greater than that of the temperature-only case. Fig 4 indicates that at moderate values of temperature and concentration, there are values of the fluctuations that cause the amplification ratio of the combined case to become less than that of the temperature-only case. This trend is continued in fig 5, where the amplification ratio of the former is always less than that of the latter. In all these figures, both cases show an increasing amplification ratio with increasing fluctuations. In fig 6 for $\overline{t} = 0.6$, the amplification ratio of the combined case at first increases, reaches

a relative maximum, then decreases as the fluctuations increase. With $\bar{T} = 0.7$, the amplification ratio of the combined case is less than unity and decreases with increasing fluctuations. The amplification ratio of the temperature-only case is greater than that of the combined case for both values of \bar{T} and increases with increasing fluctuations. Inspection of all these figures shows that the amplification ratios of both cases decrease with increasing temperature and a corresponding decrease in concentration, at constant values of fluctuations. The following is a postulated explanation for the behavior of the combined case amplification ratio.

As previously shown (refs 1 and 4), the effect of temperature fluctuations is to amplify the Arrhenius reaction rate constant. The consideration of the effects of concentration fluctuations on the reaction rate involves two factors which are in addition to this temperature effect. These factors are the probability of collision between molecules of fuel and oxidizer and the time available for two adjacent molecules of these types to react. A proper combination of these two factors allows the reaction to occur.

At low values of temperature and correspondingly high values of concentration, the fluctuations of concentration provide an amplification effect that is in addition to the amplification effect of the temperature fluctuations. This effect increases as the fluctuations increase (fig 2). This may be interpreted in terms of a higher effective concentration. While the molecules of fuel and oxidizer are spending less time, on the average, in individual collision volumes, there is a high enough concentration of them so that the probability of collision is very high, on the average, and leads to a resultant high overall probability of reaction. Thus, as a result of the increasing concentration fluctuations, the probability of collision increases more than the probability of molecules spending enough time in their collision volumes decreases. As the temperature increases and the concentration decreases, this effect is re-

duced (fig 3). That is, the probability of collision is not as large as at higher concentrations. Up to this point, the amplification effect of the concentration fluctuations is still in addition to that of the temperature fluctuations. Hence, the amplification ratio of the combined case is greater than that of the temperature-only case. The amplification ratios of both cases increase with increasing fluctuations. At some point, the value of concentration is not high enough, and an increase in the fluctuations causes the amplification ratio of the combined case to become less than that of the temperature-only case (fig 4). This is because the effect of the concentration fluctuations at this value of concentration is to cause a very low probability of two molecules spending enough time in the required collision volumes. This is not sufficiently countered by the increased probability of collision caused by the concentration fluctuations and temperature amplification effect. However, the temperature amplification effect is still strong enough to cause the amplification ratio to increase with increasing fluctuations. This is further demonstrated in fig 5. Eventually, the concentration and probability of collision become small enough so that at some value of the fluctuations, the amplification ratio decreases with increasing fluctuations (fig 6). Thus, at this point, the effect of the temperature fluctuations is not large enough to cause an increase in the amplification ratio with increasing fluctuations. Finally, the concentration is so small, the effect of the concentration fluctuations is to cause the mean turbulent reaction rate to become less than the corresponding laminar value. Hence, an amplification ratio less than unity results (fig 6). Therefore, in a given region of a flow, there are so few molecules of fuel and oxidizer, the probability of any two of them spending enough time in their collision volumes is very small, as is the probability of collision. This combines, despite the temperature amplification effect, to give an overall probability of reaction which is lower than the corresponding laminar value.

The situation of a mean turbulent reaction rate which is less than the corresponding laminar value has been observed through a combination of analysis and experiment in a turbulent premixed flame. This is reported in ref 6. In that case, calculation of the mean turbulent reaction rate through the solution of the fuel species probability transport equation results in much better agreement with experiment than the calculated average temperature laminar reaction rate. The actual mean turbulent reaction rate is less than the corresponding laminar value and the use of the probability transport equation predicts this to be so.

Shown in fig 7 is the variation of the amplification ratio with the maximum temperature, for the case of combined temperature and species fluctuations. As seen from the figure, a change in the maximum temperature can cause a very substantial change in the amplification ratio. An increased maximum temperature causes a decrease in the amplification ratio. This behavior is similar at various values of \bar{t} and $\overline{x_{H_2}}$.

In fig 8 is the variation of the amplification ratio with the correlation coefficient, for the case of combined temperature and species fluctuations. As shown, an approximate increase of twelve percent (-0.9 to -0.8) causes only a very small change in the amplification ratio. The change which does occur is a decrease in the amplification ratio. This behavior is similar at various values of \bar{t} and $\overline{x_{H_2}}$. Figs 9 and 10, comparing $\rho = -0.9$ and $\rho = -0.5$, further illustrate the relative lack of sensitivity of Z' to the correlation coefficient.

Fig 11 shows the variation in the amplification ratio with a change in the relationship between $\overline{x_{H_2}^2}$ and $\overline{t^2}$ for the case of combined temperature and species fluctuations. As demonstrated, an approximate change of thirty percent ($2/3$ to $1/2$) causes only a slight change in the amplification ratio. In general, the reduced concentration fluctuations result in a smaller amplification ratio. This be-

havior is similar at various values of \bar{t} and $\overline{x_{H_2}}$.

The results represented by Figs 2 through 11 may be summarized by the following conclusions:

1. The reaction rate amplification ratio of the combined case may be greater than, equal to or less than, that of the temperature-only case.
2. The amplification ratio of the combined case increases with increasing temperature and species concentration fluctuations, at low values of temperature and correspondingly high values of concentration. At high values of temperature and correspondingly low values of concentration, it decreases with increasing fluctuations. Thus, the model employing the modified bivariate Gaussian pdf predicts that at an initial stage of a reaction (low temperature and high concentration) the combined case mean turbulent reaction rate will be greater than the corresponding laminar value. As a reaction proceeds, this mean turbulent reaction rate will become less than the corresponding laminar value.
3. The amplification ratio of the combined case shows some sensitivity to changes in the value of maximum temperature. Hence, this value must be carefully selected.
4. The amplification ratio of the combined case is relatively insensitive to : (a) small changes in the correlation coefficient, (b) moderate changes in the relationship between temperature and species fluctuations.

3. The "Most-Likely" PDF

A joint pdf alternative to the modified bivariate Gaussian discussed in Section 2 is that suggested by Pope ⁽¹⁵⁾ and is termed the "most-likely" pdf. The single-variable form of this pdf is

$$p(t) = \exp[\lambda_0 + \lambda_1 t + \lambda_2 t^2] \quad (11)$$

where the λ 's are obtained from the following constraint equations:

$$\int_0^1 p(t) dt = 1 \quad (12)$$

$$\bar{t} = \int_0^1 t \cdot p(t) dt \quad (13)$$

$$\overline{t'^2} = \int_0^1 (t - \bar{t})^2 \cdot p(t) dt \quad (14)$$

Hence, knowledge of, say, the mean dimensionless temperature and the mean square temperature fluctuations permits a determination of λ_0 , λ_1 , and λ_2 using eqs (12), (13) and (14). Currently, this one-variable form is under investigation for comparison with the results obtained using the beta and ramp pdf's.

Multi-variable forms of the most-likely pdf are:

Two-variable

$$p(x_1, x_2) = \mathcal{Q} \cdot \exp[\lambda_0 + \lambda_1 x_1 + \lambda_2 x_2 + \lambda_3 x_1 x_2] \quad (15)$$

Three-variable

$$p(x_1, x_2, x_3) = \mathcal{Q} \cdot \exp[\lambda_0 + \lambda_1 x_1 + \lambda_2 x_2 + \lambda_3 x_3 + \lambda_4 x_1 x_2 + \lambda_5 x_1 x_3 + \lambda_6 x_2 x_3] \quad (16)$$

In eq (15), λ_0 thru λ_3 are determined from the constraint equations:

$$\int_0^1 \int_0^1 p(x_1, x_2) dx_1 dx_2 = 1 \quad (17)$$

$$\bar{x}_1 = \int_0^1 \int_0^1 x_1 \cdot p(x_1, x_2) dx_1 dx_2 \quad (18)$$

$$\bar{x}_2 = \int_0^1 \int_0^1 x_2 \cdot p(x_1, x_2) dx_1 dx_2 \quad (19)$$

$$\overline{x_1' x_2'} = \int_0^1 \int_0^1 (x_1 - \bar{x}_1)(x_2 - \bar{x}_2) \cdot p(x_1, x_2) dx_1 dx_2 \quad (20)$$

In eq (16), λ_0 thru λ_6 are determined from equations equivalent to eqs (17) thru (20) for \bar{x}_1 , \bar{x}_2 , \bar{x}_3 , $\overline{x_1' x_2'}$, $\overline{x_1' x_3'}$, $\overline{x_2' x_3'}$, and

$$\int_0^1 \int_0^1 \int_0^1 p(x_1, x_2, x_3) = 1$$

The term q in eqs (15) and (16) is an "a priori" probability whose two-variable form is

$$q = (\overline{x_1' x_2'})^{-\frac{1}{2}} \left[(1 + X) \right]^{-1} \quad (21)$$

where X is the ratio of the time scale of the turbulence to the time scale of the reaction; ie,

$$X = \frac{\tau_T}{\tau_R} \quad (22)$$

where $\tau_T = \kappa/\epsilon$, where κ is the turbulence kinetic energy and ϵ its dissipation rate. A determination of the reaction time scale, τ_R is less clear-cut. In ref 20, Pope's selection is arbitrary and unexplained. One way of formulating this term at a particular point in a turbulent flow field might be to construct an "effective half-life time" at that point from

$$\tau_R = \frac{1}{k \bar{c}} \quad (23)$$

where k is the rate constant obtained by averaging the rate constants previously obtained at neighboring points in the flow and \bar{c} is an average molar concentration obtained at those neighboring points. For example, for the bimolecular elementary reaction $A + B = C + D$, $\bar{c} = (\bar{c}_A \bar{c}_B)^{1/2}$, where \bar{c}_A and \bar{c}_B are turbulent mean values obtained at neighboring points.

The covariance, eq (20), may be obtained either from a transport equation or, more simply, from the relationship

$$\overline{x_1' x_2'} = \rho (\overline{x_1'^2})^{1/2} (\overline{x_2'^2})^{1/2} \quad (24)$$

where ρ is, as in Section 2, the correlation coefficient. Since the results obtained using the modified bivariate Gaussian were relatively insensitive to the value of ρ , a value of $\rho = 0.9$ is recommended as an initial estimate.

The formulation discussed above requires, therefore, a knowledge of first and second moments; that is, \bar{x}_1 , \bar{x}_2 , $\overline{x_1^2}$ and $\overline{x_1^2}$, along with an estimate of the parameter X in eq (21). The manner in which this analysis would be incorporated into a large-scale computer program describing turbulent reacting flows is discussed in Section 5. The three-variable formulation closely parallels the two-variable problem outlined above and will be discussed in detail in the next Status Report.

4. A Criterion for Selecting a Temperature PDF in Turbulent Flows

On the basis of comparative studies which represented turbulent temperature fluctuations by "clipped" Gaussian, beta and temperature-ramp pdf's (refs. 1 and 4), it was concluded that amplification ratios are substantially higher in regions exhibiting ramp-like behavior.

It is anticipated that in complex turbulent flow fields, regions will frequently exist in which ramp-like temperature fluctuations will be present. Outside these regions, temperature fluctuations may be best represented by, for example, the beta pdf. Hence, a criterion is required for selecting an appropriate temperature pdf when making calculations describing turbulent reacting flows. Such a criterion is developed in this Section.

Temperature fluctuations which exhibit a ramp-like structure have been observed experimentally under various flow conditions. Fiedler⁽⁷⁾ studied a heated two-dimensional mixing layer, i.e., the higher velocity stream was heated while the external stream had zero velocity and was at ambient temperature. A turbulent heated jet with a coaxial flowing stream was investigated by Antonia, Prabhu, and Stephenson.⁽⁸⁾ La Rue and Libby⁽⁹⁾, and Gibson, Chen and Lin⁽¹⁰⁾ independently studied the turbulent flow behind a heated cylinder. Ramp-like temperature fluctuations were observed in all four investigations. Despite the fact that all these experiments were performed in non-reacting flows, it is assumed that these results can be generalized to reacting flows since ramp-like fluct-

uations were observed under a wide variety of conditions likely to be encountered in reacting flows. Gibson et al. believed these types of fluctuations are due to sharp thermal gradients, with the point of highest temperature of the ramp occurring at either the downstream or upstream end of the turbulent/irrotational interface depending on the sign of the vorticity of the main flow.

Experimentally obtained temperature signals are shown in fig 12 (7), (8), (10). Note the similarity of the ramp-like structure of the signals even though they were obtained under different flow situations.

Fig 13 shows data obtained by Fiedler (7). The ordinate is the flatness factor F (also called Kurtosis) and the abscissa is a normalized distance. Note that there is a horizontal line through $F=3$ labeled "Gaussian distribution," since the Gaussian pdf has the singular value of 3 for the flatness factor. It possesses a singular value since there are no adjustable constants, as there are in the ramp pdf.

The general trend of the flatness factor in fig 13, is that it has a value of approximately 3 at the centerline ($\eta = 0$), decreases to a value near 2, then sharply increases in the outer edge of the flow field. The same trend was obtained by Antonia et al. (8), as shown in fig 14. The distance parameter is not the same as Fiedler's due to the use of different normalizing constants. Note the similarity between the figs 13 and 14. This trend of the flatness factor was observed at different axial distances and for different velocity ratios. This general behavior led Fiedler to hypothesize that the value of 2 was characteristic of the "sawtooth" appearance of the temperature signals. His criterion was supported by the appearance of ramp-like temperature signals at values of η near the centerline. For positive values of η ($\eta = 0, 0.5$), the signals exhibit a definite ramp-like structure. For these values of η , the value of the flatness factor lies between 2 and 3. Antonia et al. (8) observed the same phenomenon.

Clearly then the flatness factor F can serve as the criterion for specifying when the temperature-ramp pdf should be used in a given region of a turbulent flow field. In order to specify a range of F (around $F = 2.0$) in which ramp-like temperature fluctuations will be present, an analysis will be developed to determine the moments of the ramp pdf.

It will be recalled, refs 1 and 4, that the temperature-ramp pdf is

$$P_{T^*}(t^*) = \int_{-\infty}^{\infty} P_{R^*}(r^*) \cdot P_{N^*}(t^* - r^*) dr^* \quad (25)$$

where an asterisked quantity is one which has been normalized by dividing by a constant A_a^* , an upper-case quantity is a dimensionless, temperature-related function, and a lower-case quantity is a particular value of the function. The ramp portion of the fluctuations is represented by $p_{R^*}(r^*)$:

$$p_{R^*}(r^*) = \frac{c^{\beta-1}}{\alpha'(1-r^*)} \Gamma \left[1 - \frac{1}{\beta}, c \left(\frac{1}{\alpha'} \ln \frac{1}{1-r^*} \right)^{\beta} \right] \quad (26)$$

and the Gaussian portion is:

$$p_{N^*}(t^* - r^*) = \frac{1}{\sqrt{2\pi} \sigma^*} e^{-\frac{1}{2} \left[\frac{t^* - r^*}{\sigma^*} \right]^2} \quad (27)$$

where c , β and α' are constants. The moments are given by

$$E(t^{*n}) = \int_{-\infty}^{\infty} t^{*n} \cdot P_{T^*}(t^*) dt^* \quad (28)$$

Substituting eqs (25), (26) and (27) into (28) leads to

$$E(t^{*n}) = \int_{-\infty}^{\infty} \int_{-\infty}^{\infty} t^{*n} \frac{1}{\sqrt{2\pi} \sigma^*} e^{-\frac{1}{2} \left[\frac{t^* - r^*}{\sigma^*} \right]^2} \cdot \frac{c^{\beta-1}}{\alpha'(1-r^*)} \cdot \Gamma \left[1 - \frac{1}{\beta}, c \left(\frac{1}{\alpha'} \ln \frac{1}{1-r^*} \right)^{\beta} \right] dr^* dt^* \quad (29)$$

From ref 11,

$$\int_{-\infty}^{\infty} t^{*n} \frac{1}{\sqrt{2\pi} \sigma^*} e^{-\frac{1}{2} \left[\frac{t^* - r^*}{\sigma^*} \right]^2} dt^* = r^{*n} + \left[2^{(n-2)} + (n-2) \right] r^{*(n-2)} \sigma^{*2} + 3 r^{*(n-4)} \sigma^{*4} \quad (30)$$

which is valid for $n = 1, 2, 3$ and 4 . The gamma function in eq (30) can be replaced by (11);

$$\Gamma \left[1 - \frac{1}{\beta}, c \left(\frac{1}{\alpha'} \ln \frac{1}{1-r^*} \right)^\beta \right] = \int_x^{20} (r^*)^{(a-1)} e^{-r^*} dr^* \quad (31)$$

where $a = 1 - \frac{1}{\beta}$ and

$$x = c \left(\frac{1}{\alpha'} \ln \frac{1}{1-r^*} \right)^\beta$$

As a result of eqs (30) and (31), eq (29) now becomes

$$E(t^{*n}) = \int_0^1 \frac{c^{\beta-1}}{\alpha' (1-r^*)} \left[\int_x^{20} (r^*)^{(a-1)} e^{-r^*} dr^* \right] \left[r^{*n} + \left(2^{(n-2)} + (n-2) \right) r^{*(n-2)} \sigma^{*2} + 3 r^{*(n-4)} \sigma^{*4} \right] dr^* \quad (32)$$

where the integration limits have been changed to reflect the range of r^* .

A Monte Carlo random variable integration technique was employed to carry out the required integrations. Results for the flatness factor, F , are shown in figs 15 through 18 for the following ranges of the constants:

$$\begin{aligned} 1.7 &\leq \alpha' \leq 1.9 \\ 0.1 &\leq \sigma^* \leq 0.5 \\ 0.75 &\leq c \leq 1.25 \\ 1.0 &\leq \beta \leq 2.0 \end{aligned}$$

The values recommended by Antonia and Atkinson⁽¹¹⁾ are $\alpha^* = 1.8$, $\sigma^* = 0.25$, $c = 1.0$ and $\beta = 1.25$. Arbitrarily selecting values around these of $\pm 5\%$, the recommended range for the flatness factor is:

$$2.0 \leq F \leq 2.4$$

That is, within this range of F , temperature fluctuations should be represented by the temperature-ramp pdf. Outside this range of F , the beta pdf or some other appropriate pdf should be used to represent the temperature fluctuations.

The manner in which this criterion might be incorporated into a large-scale computer program testing reacting turbulent flows is detailed in Section 5 herein.

5. Discussion of Alternative Models for the Determination of Reaction Rates in Turbulent Reacting Flows

In order to place into context the models proposed in this Section, the five principal approaches of current interest will initially be discussed. The approaches referred to deal with the determination of species reaction rates in a turbulent reacting flow.

The first approach involves an expansion of the governing conservation equations of overall mass, momentum, species and energy in terms of limiting values of certain parameters. This is described in ref 12. The status of this method has advanced rapidly in recent years, but the resultant expansions are often found to be perturbations of laminar flows and thus may only apply to limited cases of turbulent flows.

The second approach simply utilizes the mean temperature (average, static or laminar) for the calculation of the Arrhenius reaction rate constant of the particular reaction under consideration. This is coupled with a modeled effect of the "unmixedness" on the reaction rate. The term "unmixedness" refers to the situation in which the turbulent fluctuations of fuel and oxidizer species are so great that reaction ceases at various points in a flow. This determination of a turbu-

lent reaction rate is utilized with existing turbulence modeling and is described in ref 5. While not entirely neglecting the effects of the species fluctuations, this approach does neglect the effect of the temperature fluctuations and other possible effects of the species fluctuations on the reaction rate. It has been shown in ref 13 by means of kinetic theory that the effective activation energy of any reaction in a turbulent flow is lower than that of the same reaction in an equivalent laminar flow (same mean temperature). This implies that the effect of the turbulent temperature fluctuations is to present to the flow a higher effective temperature and amplified Arrhenius reaction rate constant.

The third approach models the turbulent reaction rate based on observed physical phenomena in a flow. The result of the application of this method is termed the "eddy break up" model and is described in ref 14. This method lacks rigor and may be limited by an incomplete understanding of the physical phenomena involved.

The fourth approach utilizes the concept of the probability of temperature and species as being transportable quantities in a flow. The transport processes are those of molecular diffusion, turbulent mixing, etc. Thus, a transport equation, utilizing existing turbulence modeling, can be written in a general form and solved for specific flows. The resulting probability distribution can then be used in conjunction with the tools of applied probability theory to calculate the properties of a turbulent reacting flow. The modeling process is described in ref 15 and a transport equation solution procedure is described for example in ref 16. This method is attractive from a fundamental point of view but unfortunately, can require large amounts of computer time and storage. This problem arises when it is necessary to consider multistep reaction mechanisms, as is often the case. This is seen in refs 17 and 18, in which predictions of nitric oxide formation in the turbulent exhaust from gas turbine combustors are

made and in ref 5, where it is necessary to consider a twenty-five elementary reaction mechanism for the supersonic combustion of hydrogen with oxygen.

The fifth approach is similar in principle to that just described and has been the subject of the present study. However, instead of solving a transport equation for probability, a specific probability density function (pdf) is assumed in particular regions of a turbulent, reacting flow field and the mean turbulent reaction rate is then determined. This method is attractive as a solution to the problem of turbulent reacting flow prediction because of its basis in a fundamental physical concept and its relative computational simplicity.

Within the framework of this "presumed pdf method" (17), three models (at least) may be formulated for the reaction rate:

I. A model which assumes statistical independence between temperature and species fluctuations, in which temperature fluctuations are represented by appropriate pdf's in the various regions of the flow and the effects of species fluctuations, are treated using "unmixedness" criteria (5) or some other equivalent formulation.

II. A three-variable model which assumes statistical independence between temperature and species fluctuations, but in which the latter are treated using a joint pdf. Thus, for example, for a reaction rate term of the form:

$$\dot{w}_1 = k(t) c_{A_1} c_{A_2}$$

this model yields a mean turbulent reaction rate given by:

$$\overline{\dot{w}_1} = \left[\int_0^1 k(t) p(t) dt \right] \left[c_{A_1, \max} \cdot c_{A_2, \max} \int_0^1 \int_0^1 x_{A_1} x_{A_2} p(x_{A_1}, x_{A_2}) dx_{A_1} dx_{A_2} \right] \quad (33)$$

where it has been assumed that $c_{A_j, \min} = 0$.

III. A three-variable model using a joint pdf for the temperature and species concentrations. The form of the reaction rate terms in this case is:

$$\overline{\dot{w}_1} = c_{A_1, \text{max}} c_{A_2, \text{max}} \int_0^1 \int_0^1 \int_0^1 K(t) x_{A_1} x_{A_2} \cdot p(t, x_{A_1}, x_{A_2}) \cdot dt dx_{A_1} dx_{A_2} \quad (34)$$

The latter two models mentioned above will now be discussed in detail.

In model II, the effect of the temperature fluctuations on the rate constant is treated using the methods discussed herein and in previous Status Reports (1), (4). In most regions of the flow, the beta pdf, for example, would be used. In regions wherein the flatness factor is in the range from 2.0 to 2.4, the ramp pdf should be used. By analogy with the temperature fluctuations, (18), (19) the flatness factor may be determined from a transport equation of the form (18):

$$\rho u \frac{\partial F}{\partial x} + \rho v \frac{\partial F}{\partial y} - \frac{1}{y^i} \frac{\partial}{\partial y} \left[(\mu_e + \mu_t) y^i \frac{\partial F}{\partial y} \right] = c_3 \mu_t \left[\frac{\partial \Theta}{\partial y} \right]^2 - c_4 \frac{\rho K^{1/2} F}{\rho} \quad (35)$$

where $\Theta \equiv \bar{t}/(\bar{t}^{\prime 2})^{1/2}$. Assuming local equilibrium exists, the generation and dissipation terms on the right-hand-side may be set equal, leading to

$$F = \frac{c_3}{c_4} \rho^2 \left(\frac{\partial \Theta}{\partial y} \right)^2 \quad (36)$$

where the equality $\mu = \rho \kappa^{1/2} \rho$ has been used. It will be recalled (19) that $\bar{t}^{\prime 2}$ can be obtained from a similar relationship:

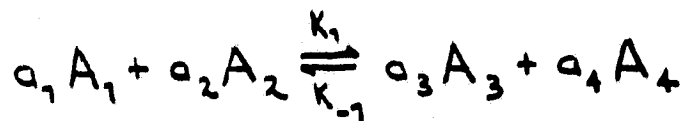
$$\overline{t^{\prime 2}} = \frac{c_1}{c_2} \rho^2 \left(\frac{\partial \bar{t}}{\partial y} \right)^2 \quad (37)$$

The constants k , c_1 , c_2 , c_3 , and c_4 must be determined empirically.

The joint pdf for the species in eq (33), $p(x_{A_1}, x_{A_2})$, might be taken to be of the modified bivariate Gaussian form (Section 2) or of the "most-likely" pdf form (Section 3). That is,

$$p(x_{A_1}, x_{A_2}) = q \cdot \exp \left(\lambda_0 + \lambda_1 x_{A_1} + \lambda_2 x_{A_2} + \lambda_3 x_{A_1} x_{A_2} \right) \quad (38)$$

where q , λ_0 , λ_1 , λ_2 , and λ_3 are obtained using the methods described in Section 3 herein. Clearly, for a chemical system of some complexity, these methods would require inordinate quantities of computer time. A preferable procedure would be to obtain in advance a tabular array or polynomial curve fits from which value of the coefficients of p can be obtained by inputting \bar{x}_{A_1} , \bar{x}_{A_2} , $\overline{x_{A_1}^2}$, $\overline{x_{A_2}^2}$, and X (the ratio of turbulent-to-reaction time scales). Then, using data from adjacent nodes, estimates of the input parameters can be used to enter the table or to use the curve fits to obtain q , λ_0 , λ_1 , λ_2 and λ_3 . The reaction rate terms are next calculated using eq (33) for each term; then the reaction rate itself is determined from the summation of the individual terms. That is, for a set of bimolecular elementary reactions of the general form



the laminar reaction rate of, say, species A_1 is

$$\dot{w}_{A_1} = -k_1 c_{A_1} c_{A_2} + k_{-1} c_{A_3} c_{A_4} - \dots$$

and the turbulent reaction rate is

$$\overline{w}_{A_1} = -\overline{w}_{1,A_1} + \overline{w}_{-1,A_1} - \dots$$

where \bar{w}_{1,A_1} is given by eq (33) and the remaining terms, \bar{w}_{-1,A_1} , \bar{w}_{2A_1} , etc. are given by expressions equivalent to eq (33). Here again, the concept of using a tabular array or curve fits will serve to eliminate the necessity for repeated integrations of eq (33). That is, after selection of the appropriate $p(t)$ using the flatness factor criterion, a table will be entered with \bar{t} , \bar{t}^2 , \bar{x}_{A_1} , \bar{x}_{A_2} , $\overline{x_{A_1}^2}$, $\overline{x_{A_2}^2}$ and X to obtain Z' :

$$Z'_{1,A_1} = \frac{\bar{w}_{1,A_1}}{\dot{w}_{1,A_1}} = \frac{\left[\int_0^1 k_1(t) p(t) dt \right] \left[\int_0^1 \int_0^1 x_{A_1} x_{A_2} p(x_{A_1}, x_{A_2}) dx_{A_1} dx_{A_2} \right]}{K_1 \bar{x}_{A_1} \bar{x}_{A_2}} \quad (39)$$

Since $\dot{w}_{1,A_1} = -k_1 x_{A_1} x_{A_2}$ is readily determined using existing procedures (5), \bar{w}_{1,A_1} and like terms can be calculated.

A major near-term task under this grant is the determination of values of $Z'(\bar{t}, \bar{t}^2, \bar{x}_{A_1}, \bar{x}_{A_2}, \overline{x_{A_1}^2}, \overline{x_{A_2}^2}, X)$.

The third model mentioned earlier is a three-variable model in which a joint pdf is employed for both temperature and species fluctuations; ie, $p(t, x_{A_1}, x_{A_2})$. In this case, the pdf will be assumed to be given by the following three-variable form of the "most-likely pdf":

$$p(t, x_{A_1}, x_{A_2}) = q \cdot \exp \left[\lambda_0 + \lambda_1 t + \lambda_2 x_{A_1} + \lambda_3 x_{A_2} + \lambda_4 t x_{A_1} + \lambda_5 t x_{A_2} + \lambda_6 x_{A_1} x_{A_2} \right] \quad (40)$$

where the method for obtaining q and the constraint equations for $\lambda_0, \lambda_1, \dots, \lambda_6$ are similar to those detailed in Section 3 herein. As with model II above, the amplification ratio $Z'_{1,A_1} = \bar{w}_{1,A_1} / \dot{w}_{1,A_1}$ can be determined a priori as a function of \bar{t} , \bar{x}_{A_1} , \bar{x}_{A_2} , $\overline{t x_{A_1}}$, $\overline{t x_{A_2}}$, $\overline{x_{A_1} x_{A_2}}$ and X and set up in the form of a tabular array or curve fits for use in large-scale computer programs.

It will be noted that the models discussed above require values of the mean square species fluctuations, $\overline{x_{A_j}^2}$, as well as the mean square temperature fluctuations. As is the case with the latter, transport equations for the species fluctuations could, conceptually, be introduced for each species as was done in ref 5 for the fuel and oxidizer. The general form is

$$\rho u \frac{\partial g_j}{\partial x} + \rho v \frac{\partial g_j}{\partial y} - \frac{1}{y^i} \frac{\partial}{\partial y} \left(\frac{\mu_t}{\sigma_{g_j}} y^i \frac{\partial g_j}{\partial y} \right) = c_{g_1} \left(\frac{\epsilon}{\kappa} \right) \left(\frac{\partial u}{\partial y} \right)^2 - c_{g_2} \left(\frac{\epsilon}{\kappa} \right) \rho g_j \quad (41)$$

where the symbols are the same as in ref 5 and $g_j \propto (\overline{x_{A_j}^2})^{1/2}$. In actual practice, computer time and space restrictions will generally militate against the addition of these differential equations, particularly when detailed chemical kinetics are involved. In light of the other uncertainties in the analysis, it is argued that a local equilibrium assumption is in order, similar to that used to obtain eq (36), in which case eq (41) reduces to

$$g_j = \frac{1}{\rho} \frac{c_{g_1}}{c_{g_2}} \left(\frac{\partial u}{\partial y} \right)^2 \quad (42)$$

Attention will be focussed during the forthcoming semi-annual period on the Model II problem discussed above. In addition, a one-dimensional, temperature-only form of the "most-likely" pdf:

$$p(t) = \exp \left(\lambda_0 + \lambda_1 t + \lambda_2 t^2 \right)$$

will be investigated for comparison with the beta and ramp pdf models.

References

1. Kassab, G.M., Antaki, P.J. and Chinitz, W., "A Comprehensive Model to Determine the Effects of Temperature and Species Fluctuations on Reaction Rates in Turbulent, Reacting Flows," Semi-Annual Status Report, 8/1/80 - 1/31/81.
2. Pope, S.B., "A Rational Method of Determining Probability Distributions in Turbulent Flows," J. Non-Equil. Thermo., 4, 1979, pp. 309-320.
3. Kent, J.H. and Bilger, R.W., "Turbulent Diffusion Flames," 14th Symp. (Intl) on Comb., 1974, pp. 615-624.
4. Chinitz, W., Antaki, P.J. and Kassab, G.M., "A Comprehensive Model to Determine the Effects of Temperature and Species Fluctuations on Reaction Rates in Turbulent, Reacting Flows," Semi-Annual Status Report, 2/1/80 - 7/31/80.
5. Evans, J.S. and Schexnayder, C.J. Jr., "Influence of Chemical Kinetics and Unmixedness on Burning in Supersonic Hydrogen Flames," AIAA Journal, 18, 2, Feb. 1980, pp. 188-193.
6. Khalil, E.E., "On the Prediction of Reaction Rates in Turbulent Premixed Confined Flames," AIAA Preprint No. 80-0015, Jan. 1980.
7. Fiedler, H., "Transport of Heat Across a Plane Turbulent Mixing Layer," Advances in Geophysics, 18, 1974, pp. 93-109.
8. Antonia, R.A., Prabhu, A. and Stephenson, S.E., "Conditionally Sampled Measurements in a Heated Turbulent Jet," J. Fluid Mech., 72, 1975, pp. 455-480.
9. La Rue, J.C. and Libby, P.A., "Temperature Fluctuations in the Plane Turbulent Wake," Phys. of Fluids, 17, 1974, pp. 1956-1967.
10. Gibson, C.H., Chen, C.C. and Lin, S.C., "Measurements of Turbulent Velocity and Temperature Fluctuations in the Wake of a Sphere," AIAA Journal, 6, 4, 1967, pp. 642-649.
11. Antonia, R.A. and Atkinson, J.D., "A Ramp Model for Turbulent Temperature Fluctuations," Phys. of Fluids, 19, 9, 1976, pp. 1273-1278.
12. Williams, F.A., "Current Problems in Combustion Research," Dynamics and Modeling of Reactive Systems, Academic Press, Inc., 1980, pp. 293-314.
13. Tsuge, S. and Sagara, K., "Arrhenius' Law in Turbulent Media and an Equivalent Tunnel Effect," Comb. Sci. and Tech., 18, 1978, pp. 179-189.
14. Spalding, D.B., "Development of the Eddy-Break-Up Model of Turbulent Combustion," 16th Symp. (Intl) on Comb., 1976.
15. Pope, S.B., "The Probability Approach to the Modeling of Turbulent Reacting Flows," Comb. and Flame, 27, 1976, pp. 299-312.

16. Pope, S.B., "Monte Carlo Calculations of Premixed Turbulent Flames," 18th Symp. (Intl) on Comb., 1980.
17. Moreau, P. and Borghi, R., "Experimental and Theoretical Studies of Nitrogen Oxide Production in a Turbulent Premixed Flame," AIAA Preprint No. 80-0078, Jan. 1980.
18. Mikatarian, R.R., "Turbulent Dissipation Effects on Chemical Laser Performance," AIAA Preprint No. 74-547, June 1974.
19. Chinitz, W., "A Model to Determine the Effects of Temperature Fluctuations on the Reaction Rate Constant in Turbulent Reacting Flows," Report submitted to the Hypersonic Propulsion Branch, NASA LaRC, Aug. 1979.
20. Pope, S.B., "Probability Distributions of Scalars in Turbulent Shear Flow," Proc, 2nd Symp. on Turbulent Shear Flows, London, 1979, pp. 3.1-3.6.

LIST OF SYMBOLS

A	pre-exponential factor, eq (7)
A_a	constant used in eq (25)
a	duct radius
B	temperature exponent, eq (7)
C	molar concentration; constant
c	constant; molar concentration; constant in eq (26)
F	flatness factor or Kurtosis
$f(x,y)$	two-variable pdf
g	rms species fluctuation
$k(t)$	Arrhenius reaction rate constant
k_1, k_2^-	constants
L	Prandtl mixing length
λ	Prandtl mixing length
$p(t)$	one-variable pdf
$p(x,y)$	two-variable pdf
q	"a priori" probability, eq (21)
r	radial coordinate
T	temperature
T_A	"activation temperature" ratio of activation energy to gas constant
t	dimensionless temperature
U	axial velocity
u, v	two-dimensional or axisymmetric velocities
v	defined in eq (2)
\dot{w}	reaction rate
X	ratio of turbulence-to-reaction time scales, eq (22)

x	dimensionless molar concentration
x, y	two-dimensional or axisymmetric space coordinates
z	rate constant "amplification ratio," eq (9)
z^1	reaction rate "amplification ratio," eq (8)
α^1	constant in eq (26)
β	constant in eq (26)
ϵ	dissipation rate of the turbulence kinetic energy
λ	parameters in the "most-likely" pdf
κ	turbulence kinetic energy
ρ	correlation coefficient; mass density
μ	Gaussian mean
σ	Gaussian rms fluctuation
θ	defined after eq (35)
τ	time

Subscripts

A_j	species index
F	fuel
l	laminar value
max	maximum value
min	minimum value
O	oxidizer
R	reaction
T	turbulent
t	dimensionless temperature; turbulent value
x	dimensionless molar concentration

Superscripts

- o initial value
- * quantity normalized by dividing by A_a

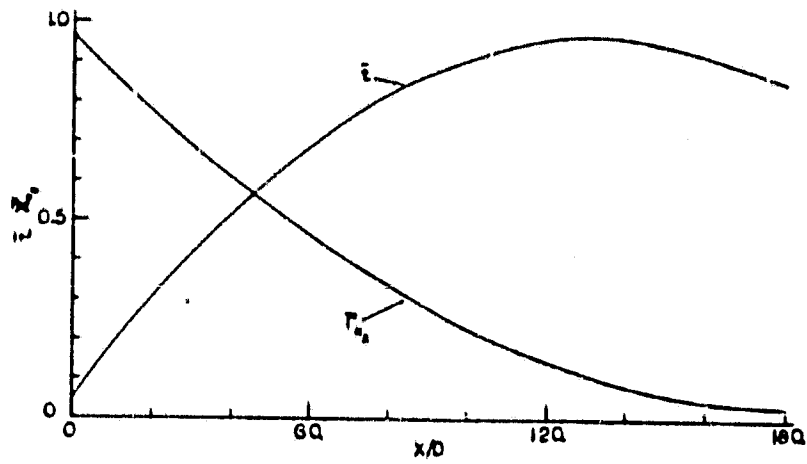


FIG. 1. Curve Fits of the Data of Kent and Bilger⁽³⁾ (Fig 2, $\bar{U}_j/U_c = 8$)

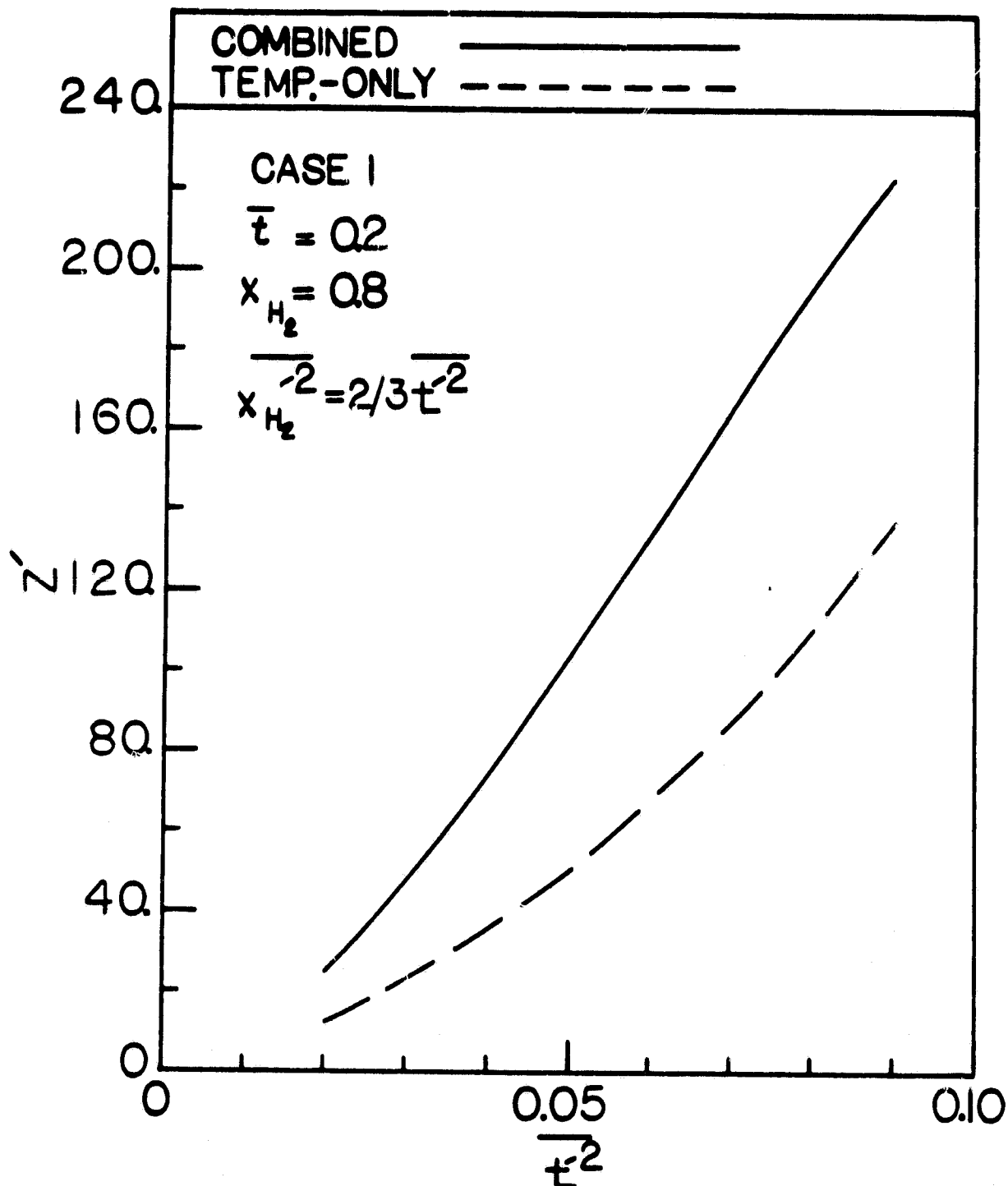


Figure 2. Variation of the reaction rate amplification ratio with temperature and species fluctuations for the combined (modified bivariate Gaussian pdf) and temperature-only (beta pdf) cases

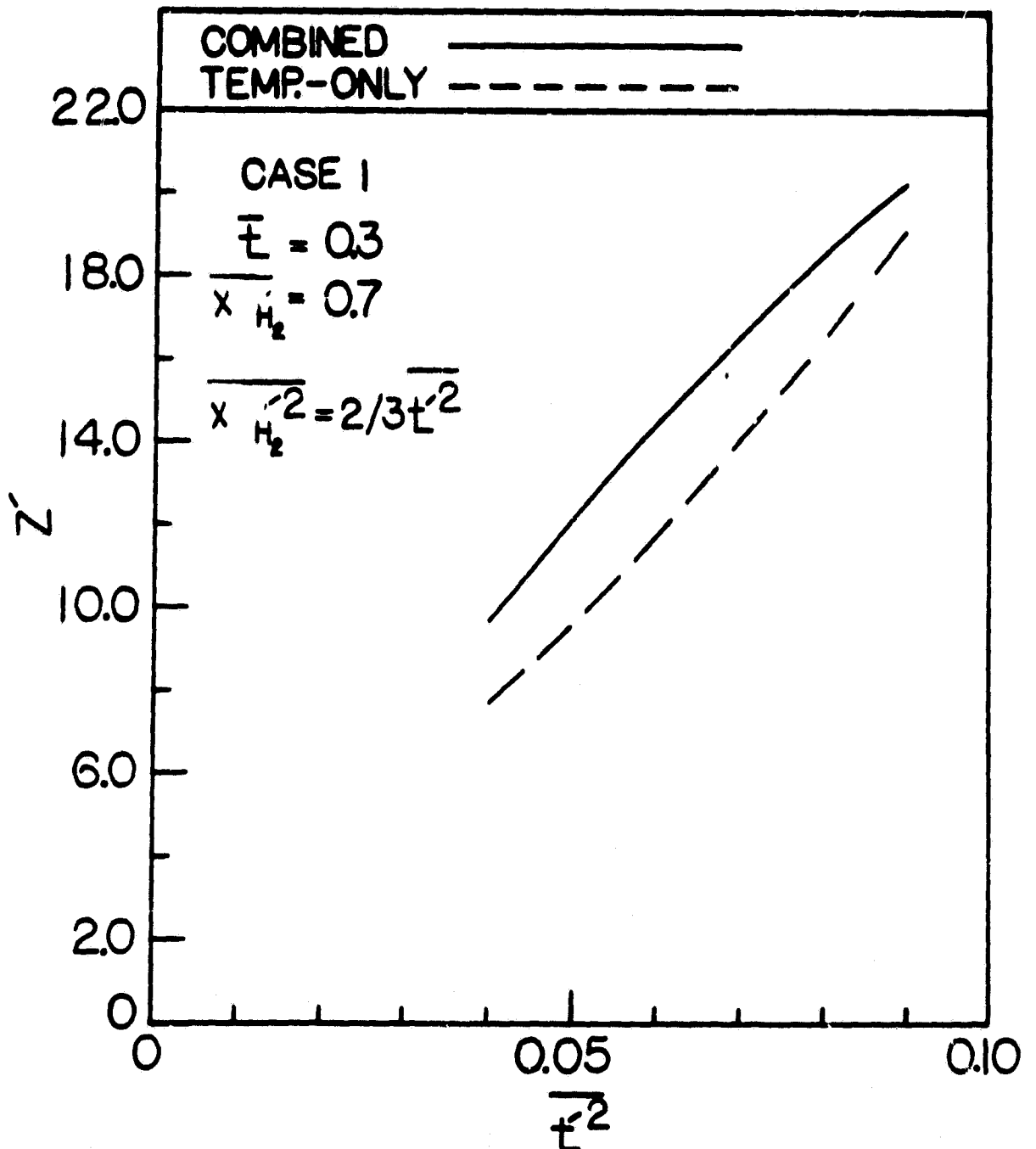


Figure 3 . Variation of the reaction rate amplification ratio with temperature and species fluctuations for the combined (modified bivariate Gaussian pdf) and temperature-only (beta pdf) cases

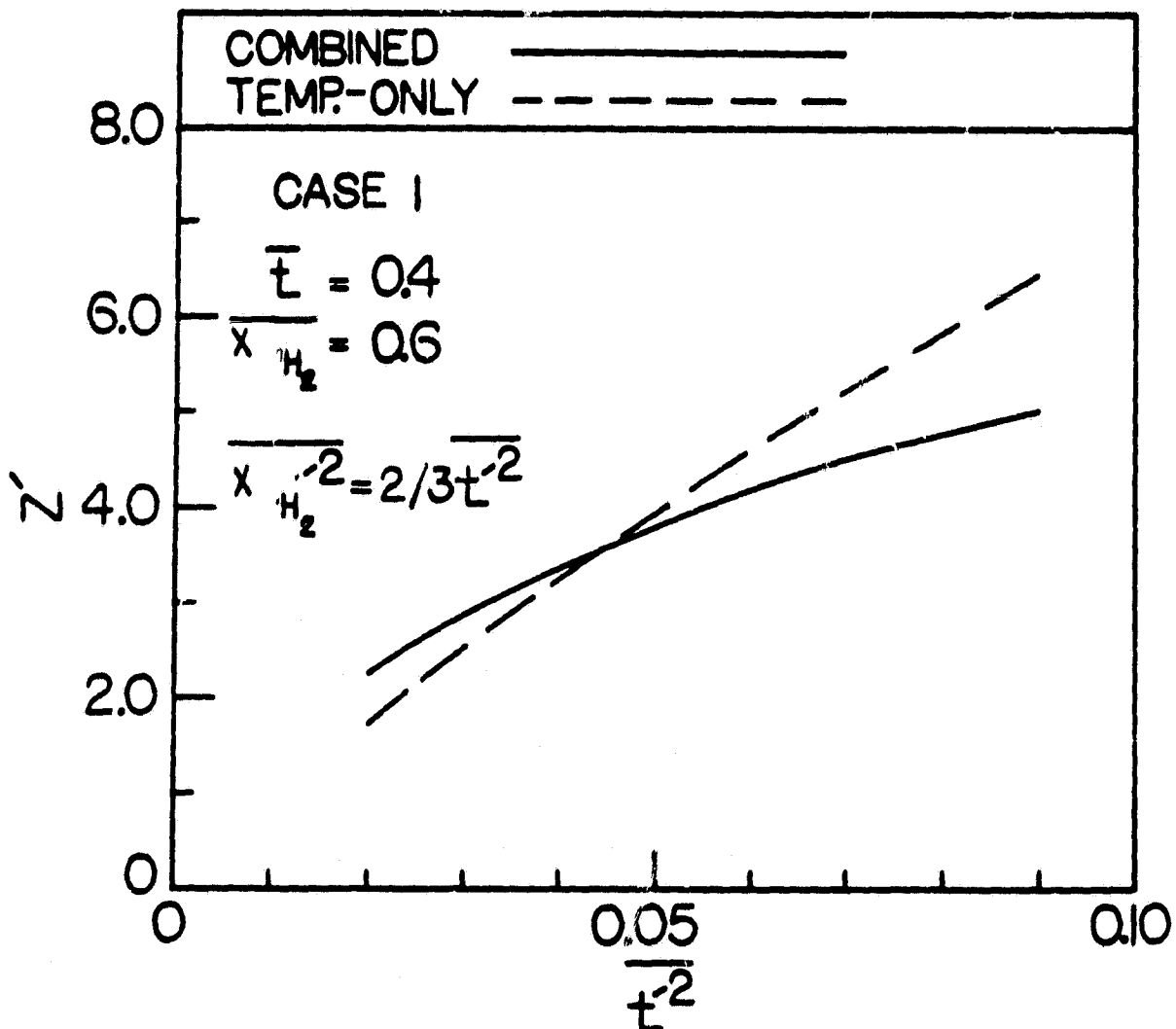


Figure 4. Variation of the reaction rate amplification ratio with temperature and species fluctuations for the combined (modified bivariate Gaussian pdf) and temperature-only (beta pdf) cases

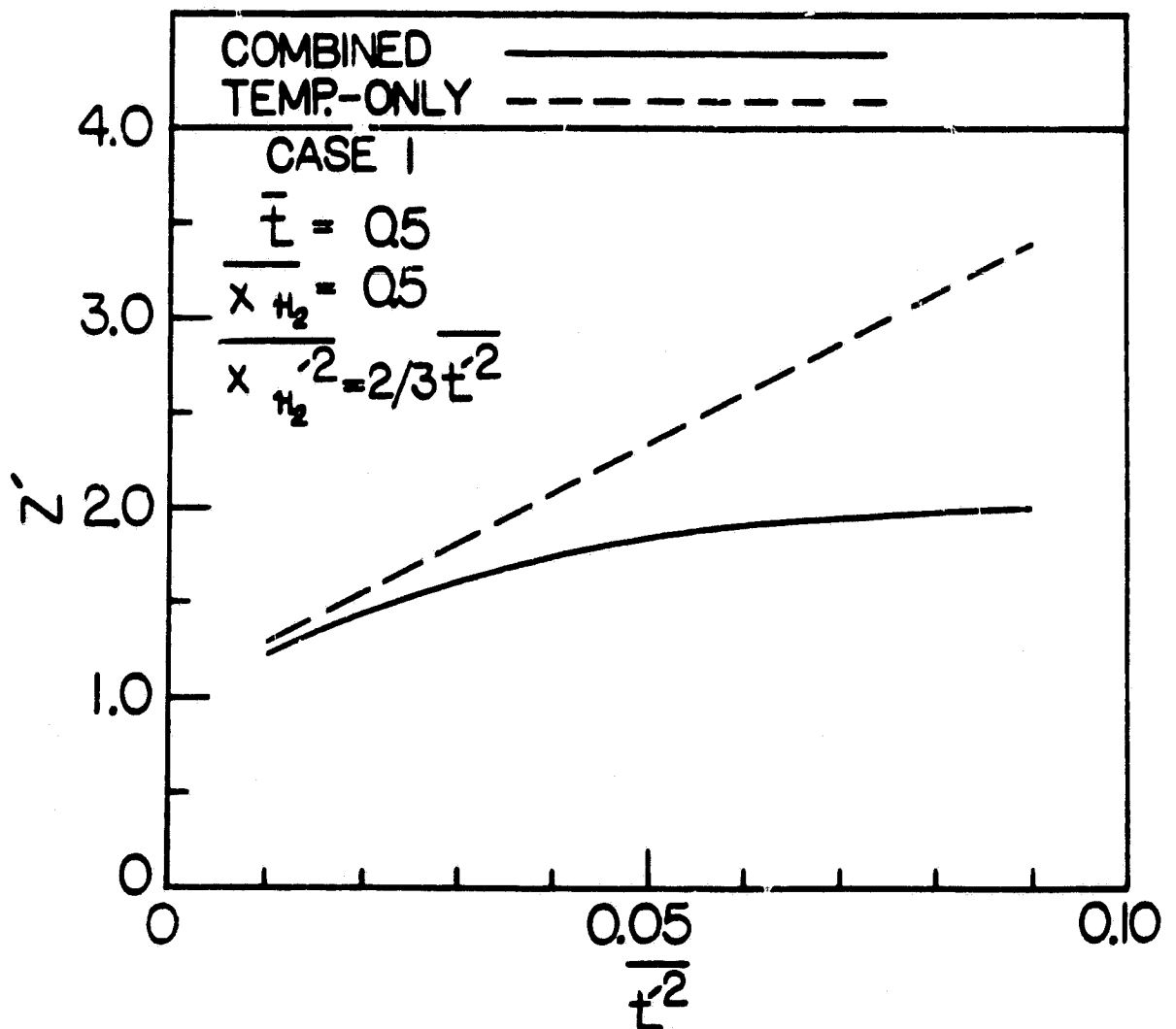


Figure 5. Variation of the reaction rate amplification ratio with temperature and species fluctuations for the combined (modified bivariate Gaussian pdf) and temperature-only (beta pdf) cases

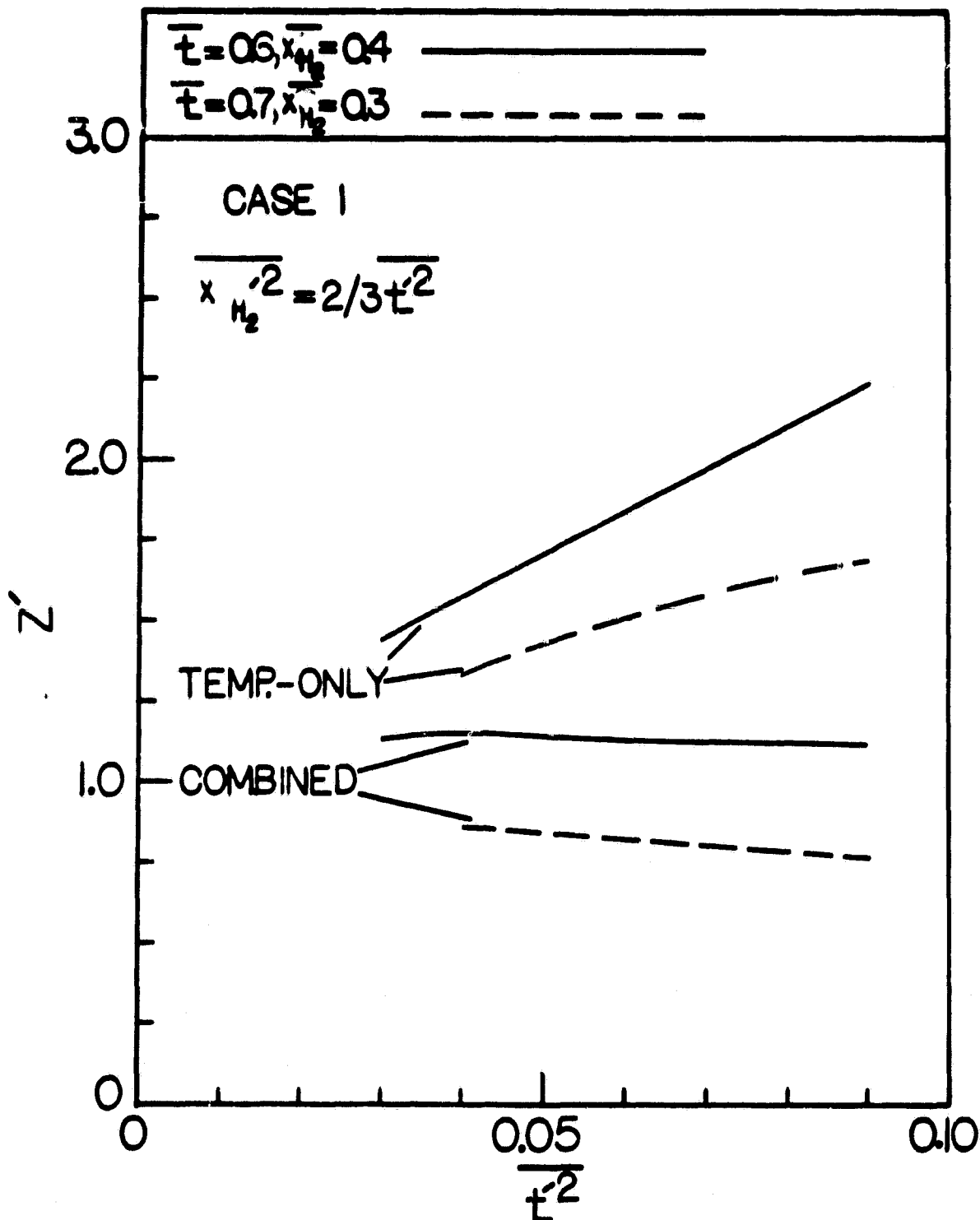


Figure 6. Variation of the reaction rate amplification ratio with temperature and species fluctuations for the combined (modified bivariate Gaussian pdf) and temperature-only (beta pdf) cases

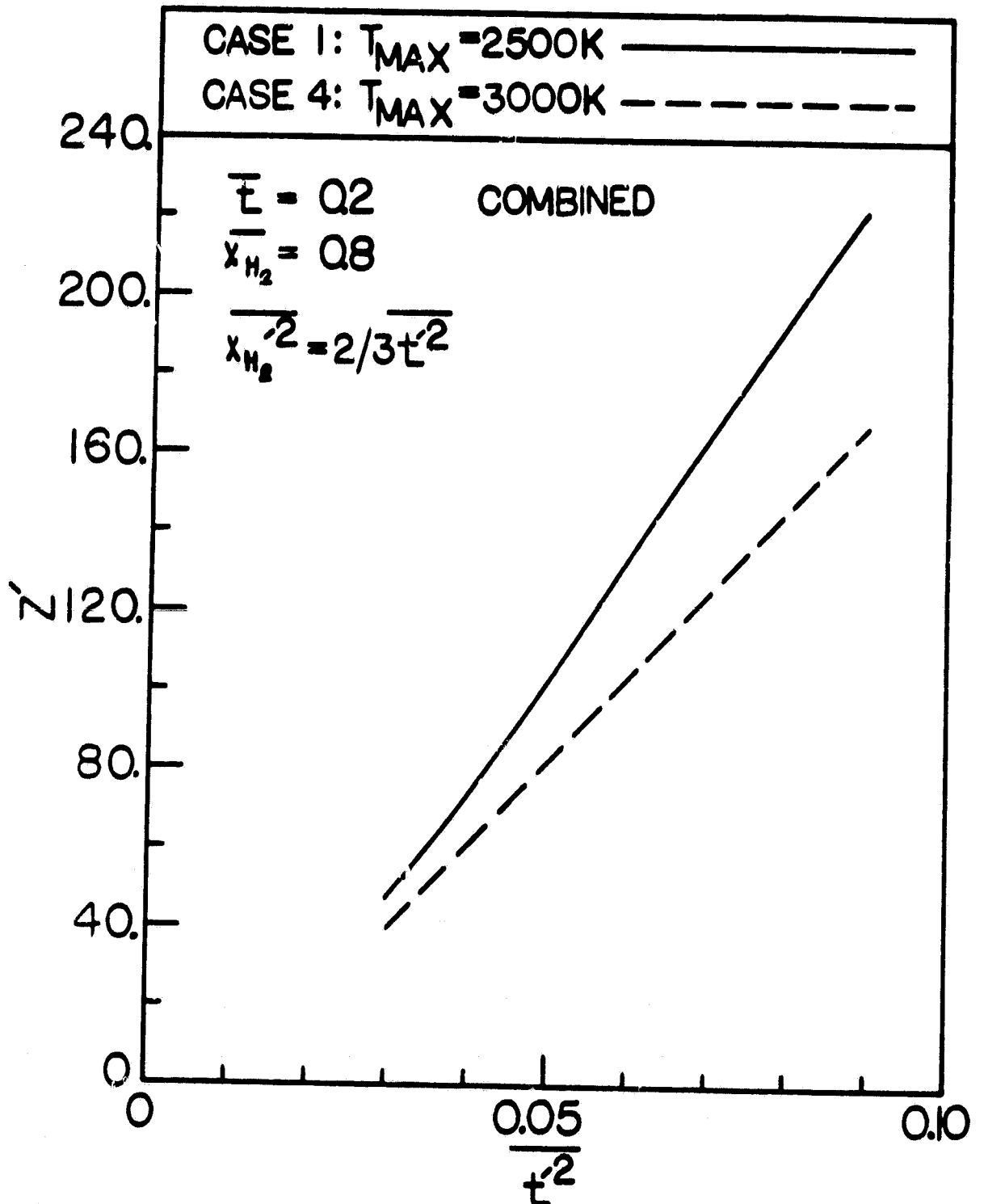


Figure 7 . Variation of the reaction rate amplification ratio with the maximum temperature for the combined case (modified bivariate Gaussian pdf)

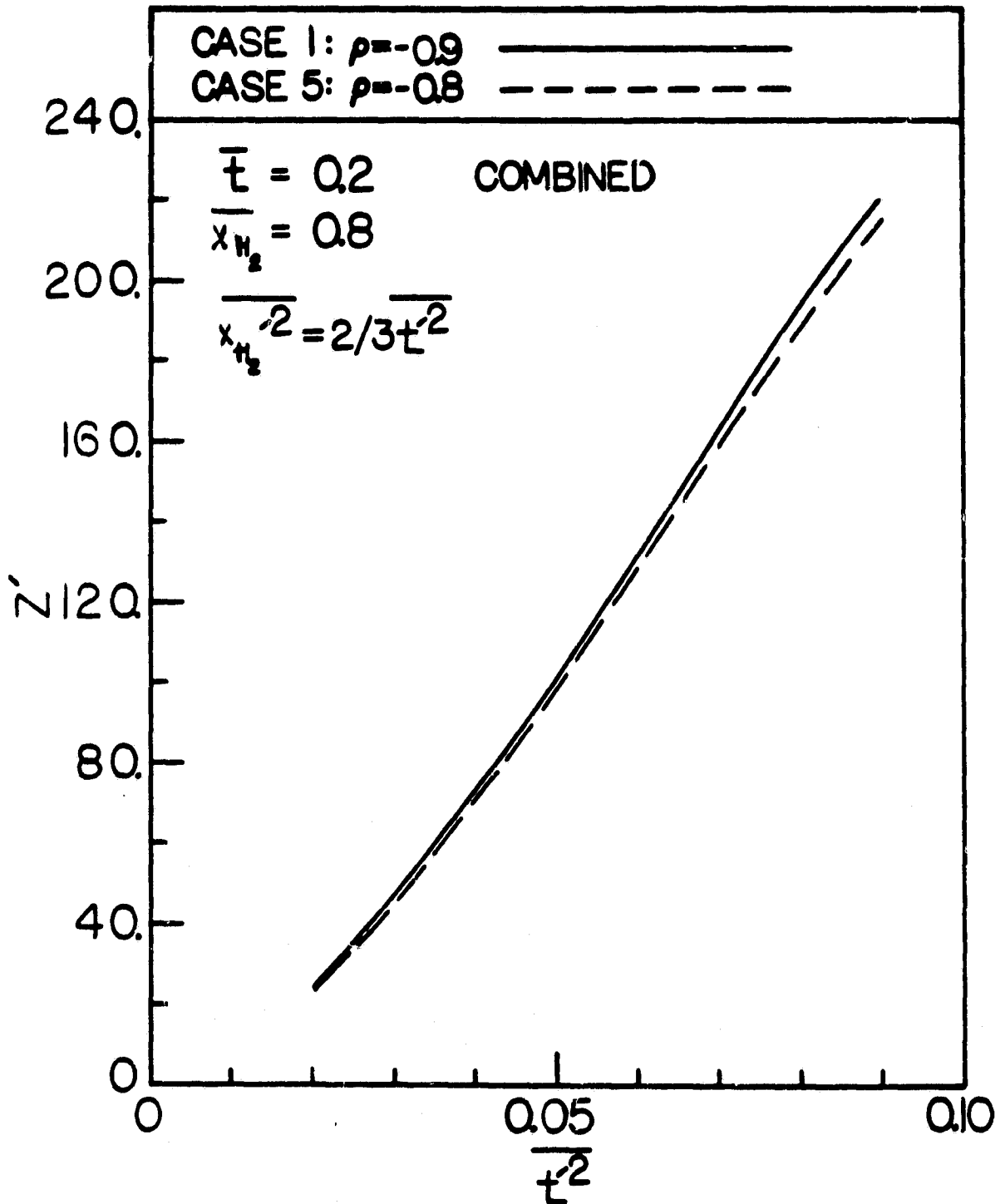


Figure 8. Variation of the reaction rate amplification ratio with the correlation coefficient for the combined case (modified bivariate Gaussian pdf)

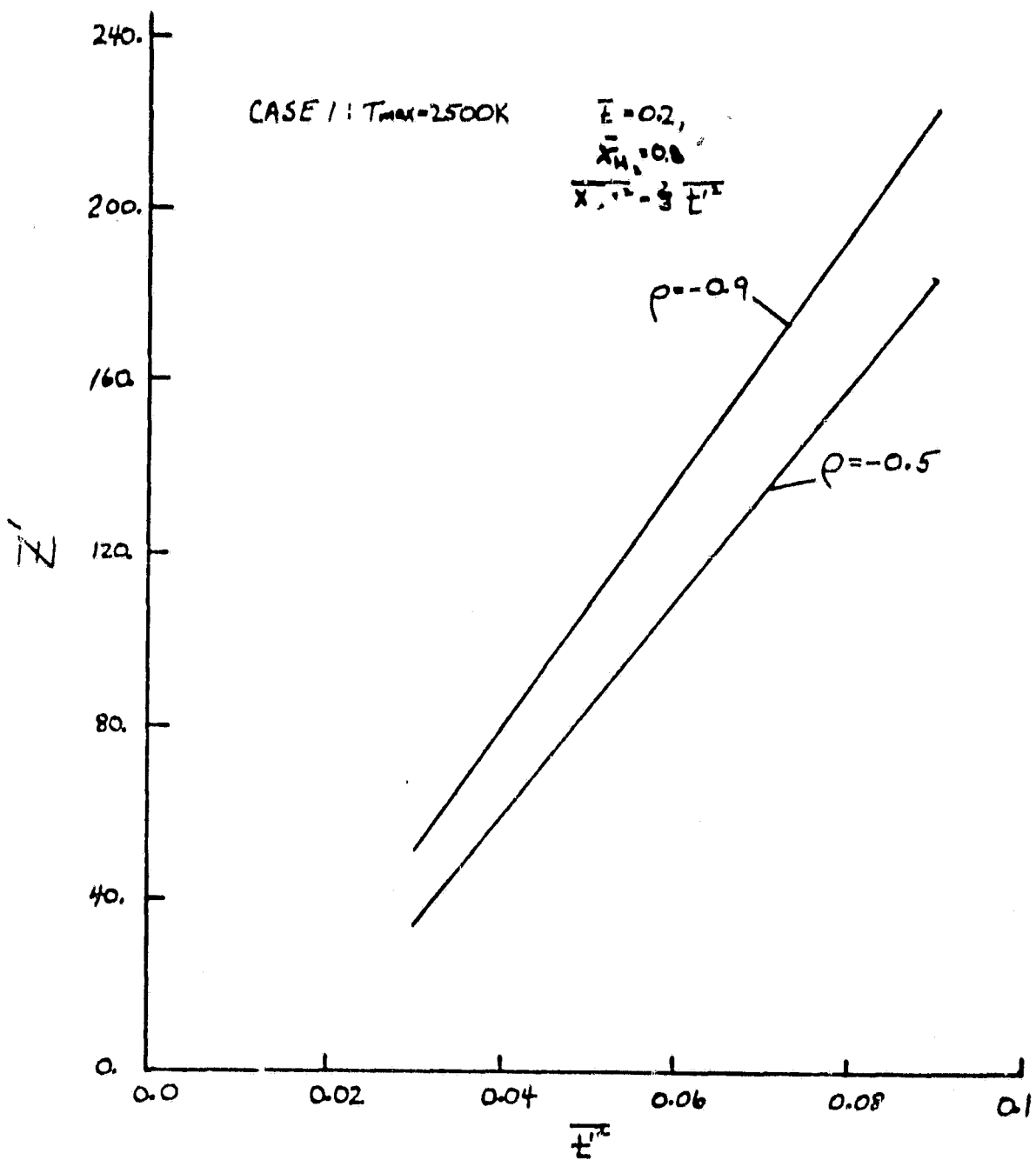


Figure 9 Reaction Rate Amplification Ratio, Z' , for Case 1, as calculated with the modified Bivariate Gaussian pdf

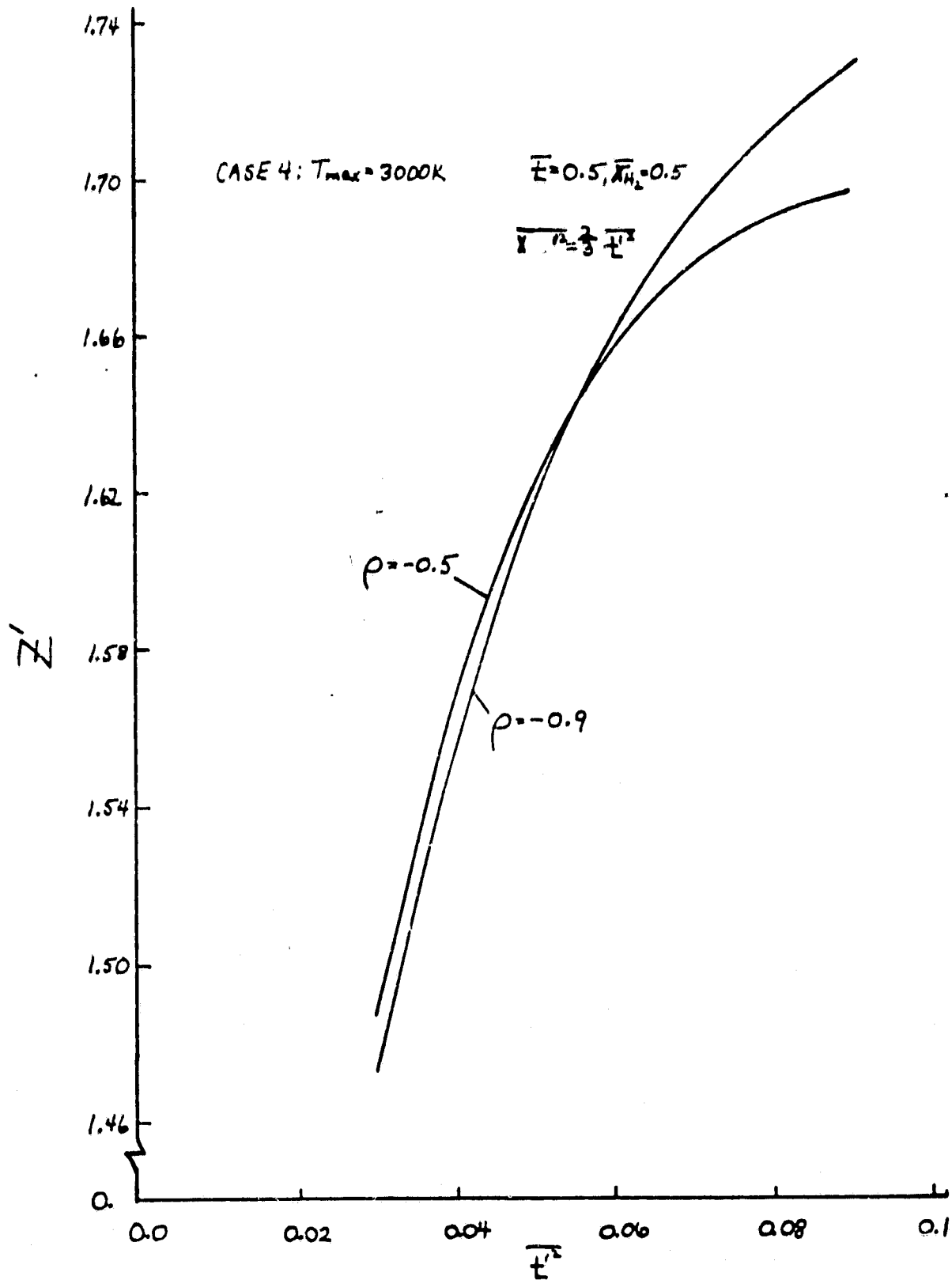


Figure 10 Reaction Rate Amplification Ratio, Z' , for Case 4, as calculated with the modified Bivariate Gaussian pdf

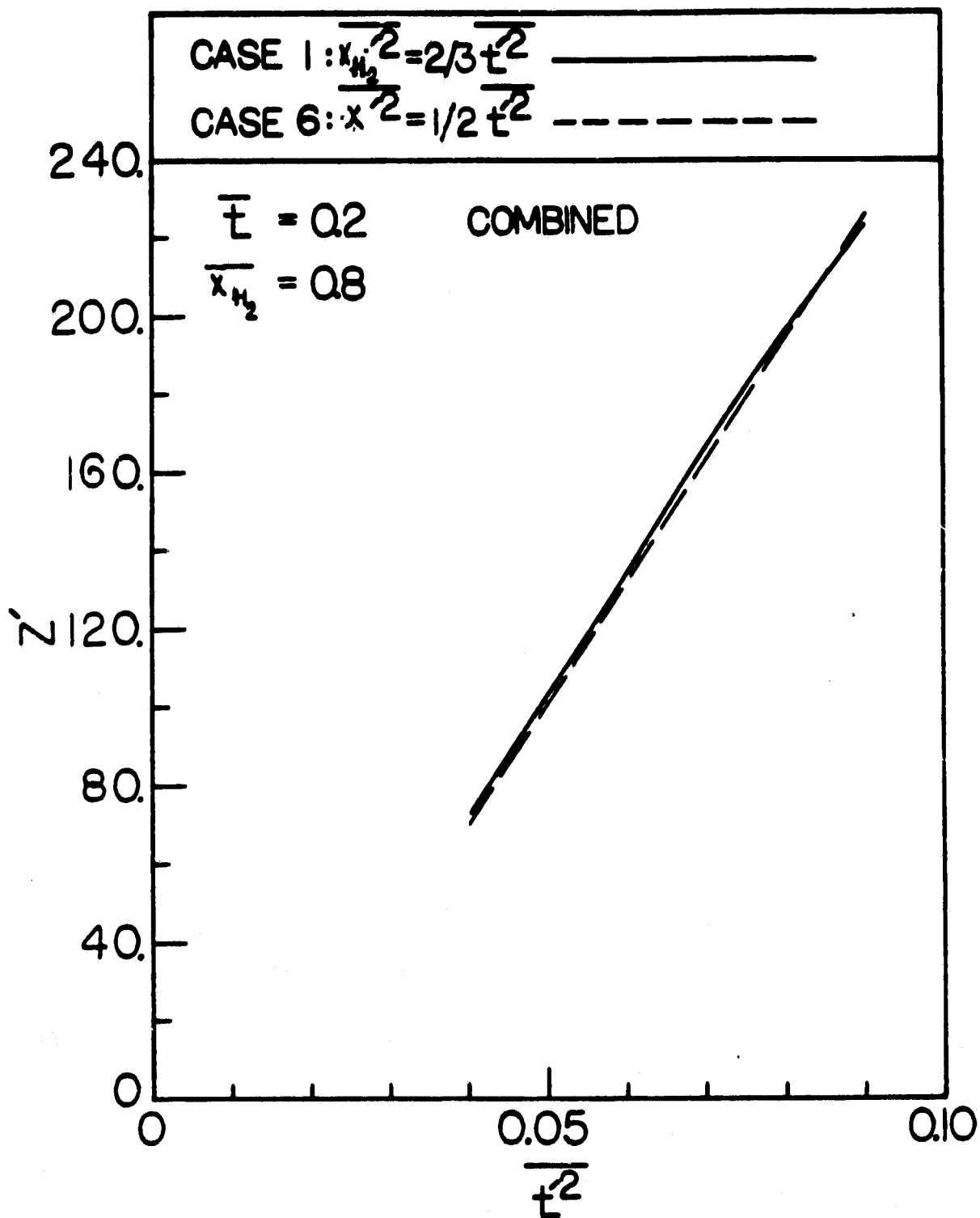
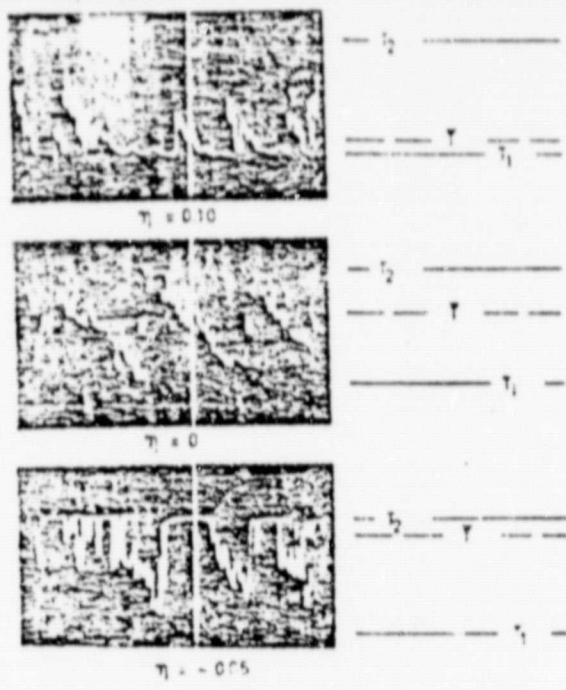


Figure 11. Variation of the reaction rate amplification ratio with the relationship between temperature and species fluctuations for the combined case (modified bivariate Gaussian pdf)

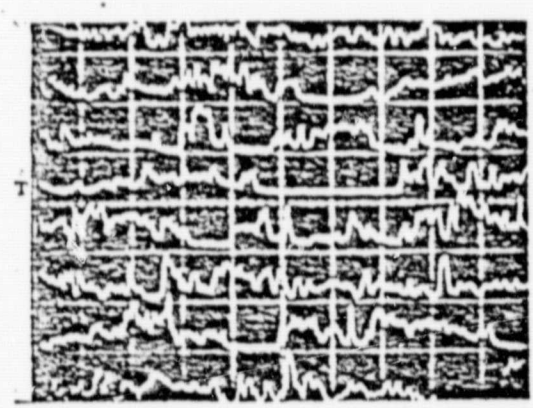


Fiedler (7)

ORIGINAL PAGE IS
OF POOR QUALITY



Antonia, et.al. (8)



Gibson, et.al. (10)

FIG 12. EXPERIMENTAL RESULTS ILLUSTRATING RAMP-LIKE TEMPERATURE FLUCTUATIONS

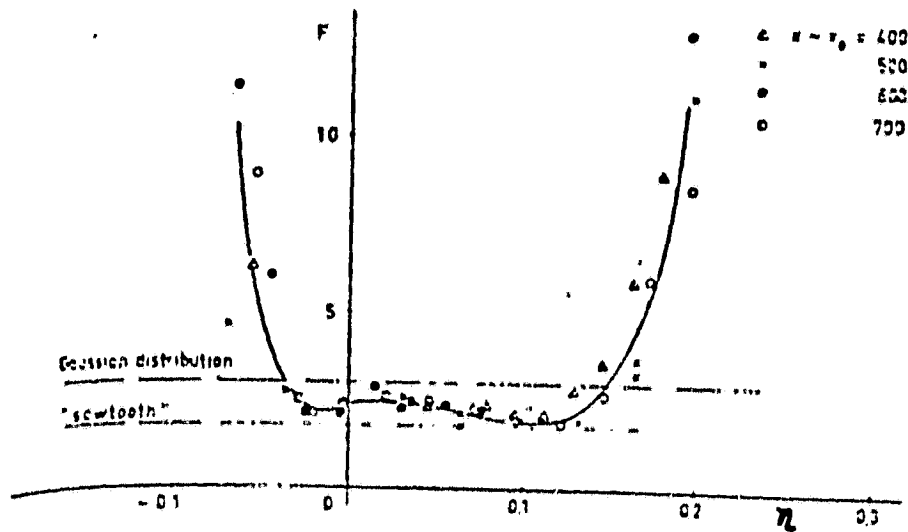


FIG 13. FLATNESS DISTRIBUTION OF TEMPERATURE
(DATA OF FIEDLER (7))

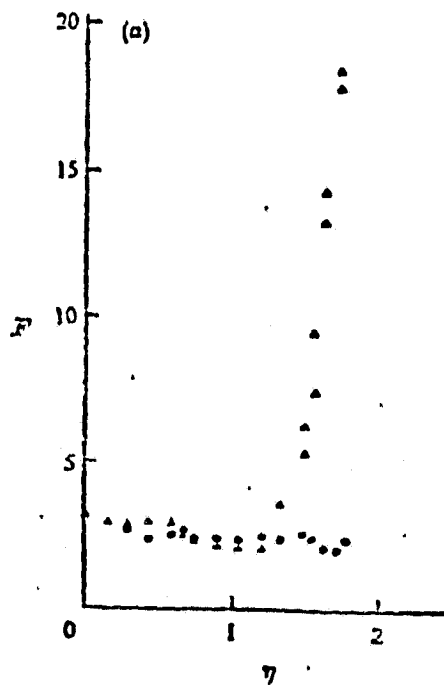


FIG 14. FLATNESS DISTRIBUTION OF TEMPERATURE
(DATA OF ANTONIA, ET. AL. (8))

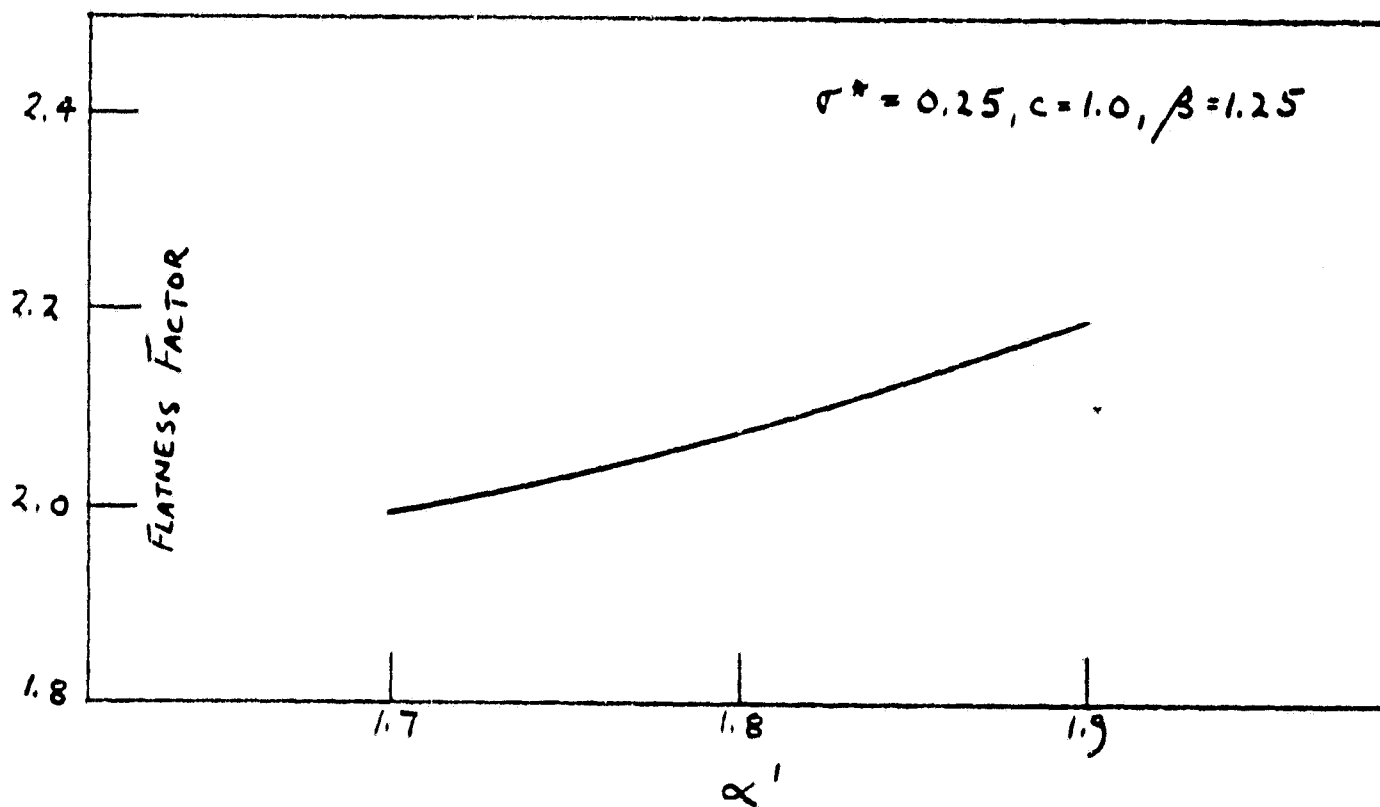


Figure 15. Flatness Factor as a Function of the "Constant" α' (Ramp PDF)

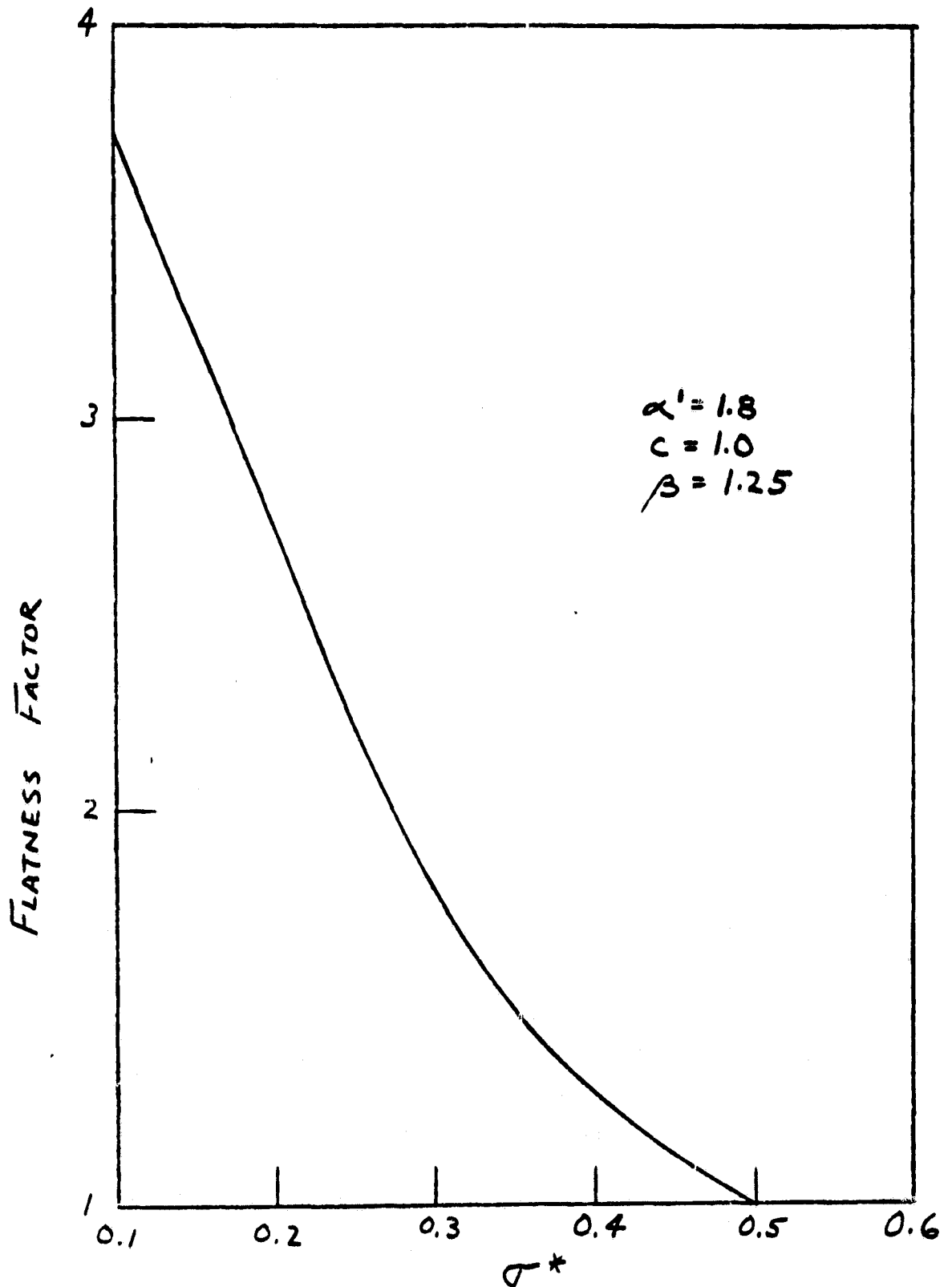


Figure 16. Flatness Factor as a Function of the Intensity of the Gaussian Fluctuations (Ramp PDF)

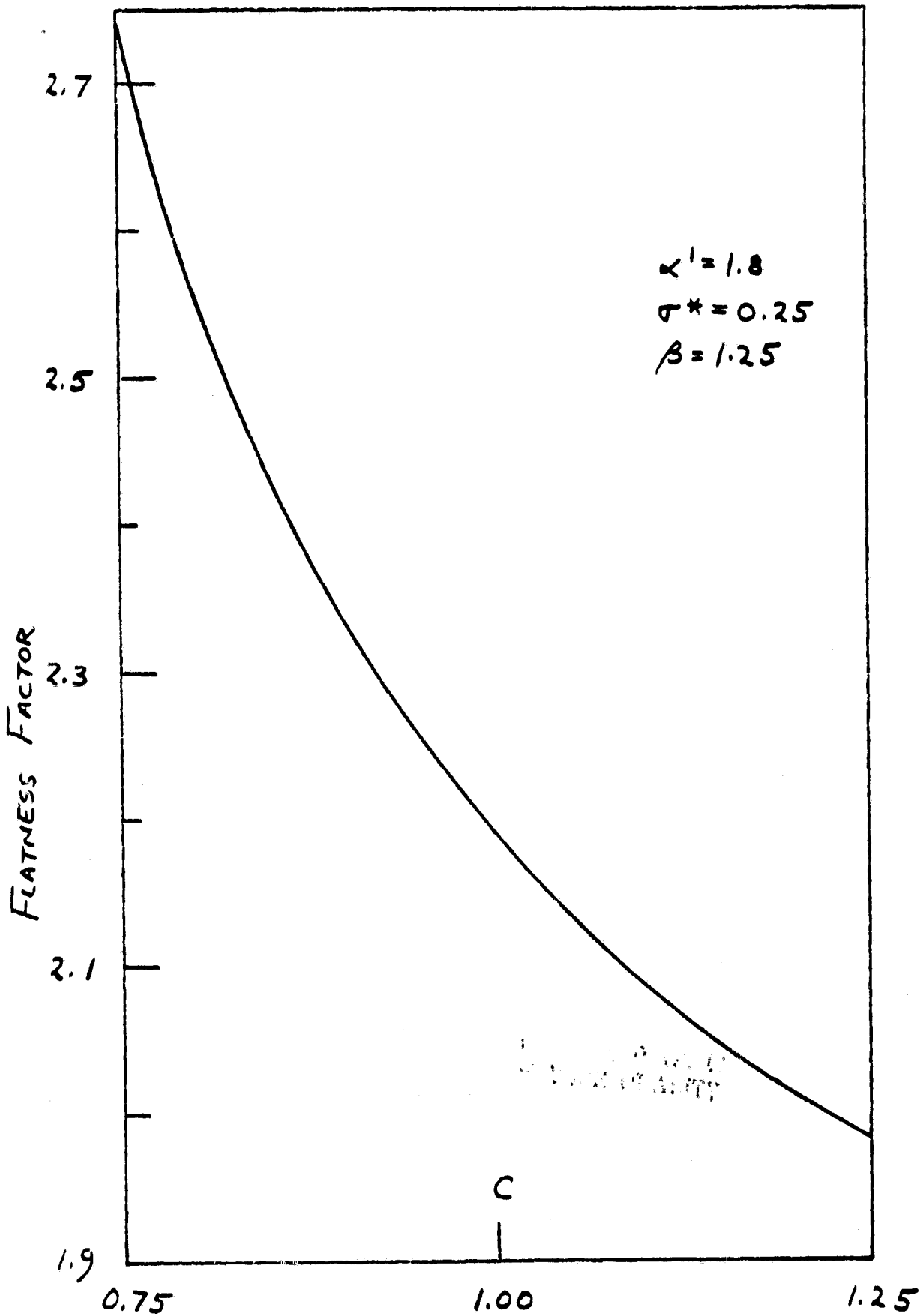


Figure 17. Flatness Factor as a Function of the "Constant" c (Ramp PDF)

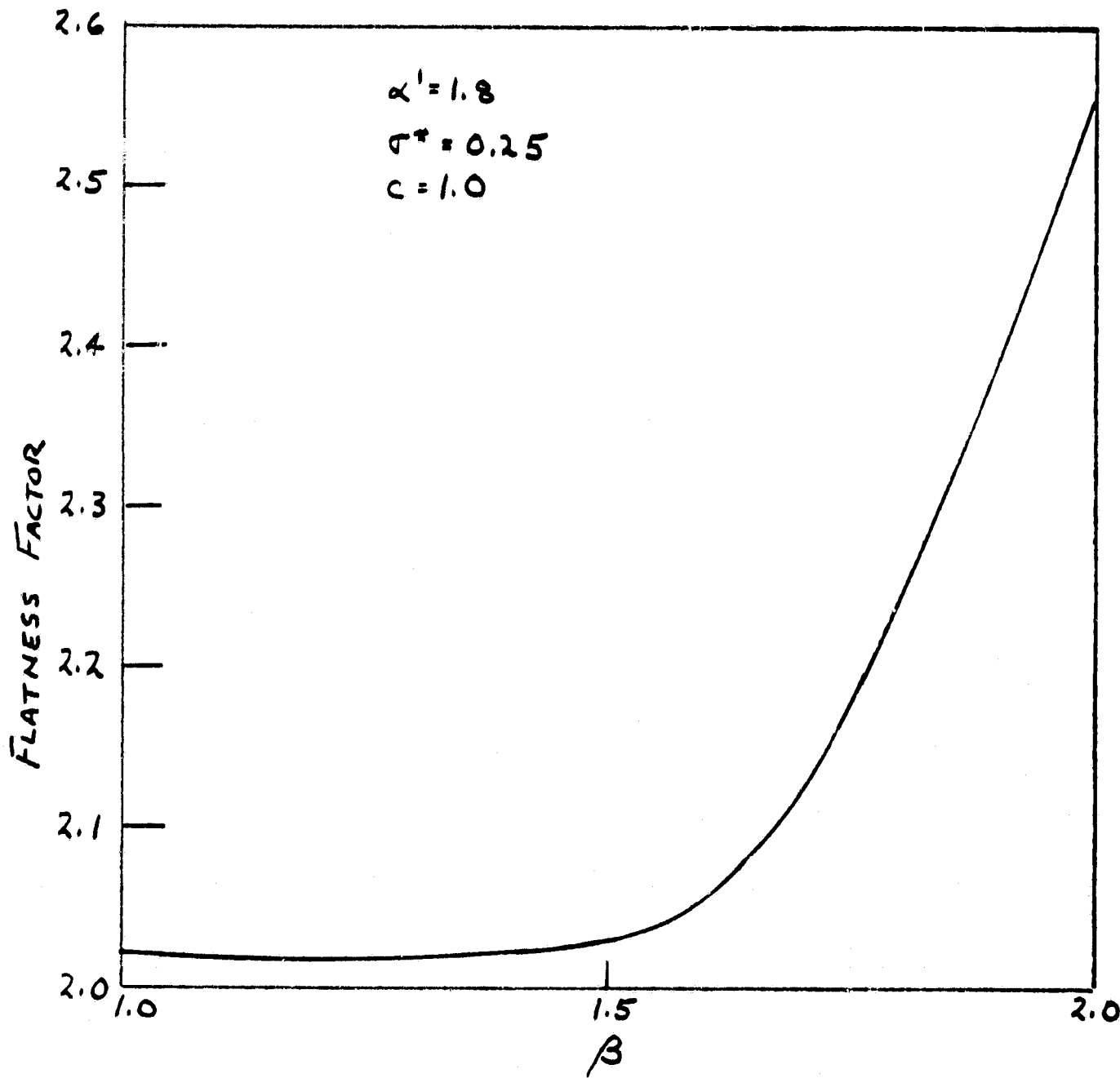


Figure 18. FLATNESS FACTOR AS A FUNCTION of the "CONSTANT" β (RAMP PDF)